Regional, multi-decadal analysis on the Loire River basin reveals that stream temperature increases faster than air temperature

Hanieh Seyedhashemi[1,2], Jean-Philippe Vidal[1], Jacob S. Diamond[1], Dominique Thiéry[3], Céline Monteil[4], Frédéric Hendrickx[4], Anthony Maire[4], and Florentina Moatar[1]

[1]INRAE, UR RiverLy, 5 rue de la Doua CS 20244, 69625 Villeurbanne, France
[2]EA 6293 GéoHydrosystèmes COntinentaux, Université François-Rabelais de Tours, Parc de Grandmont, 37200 Tours, France
[3]BRGM, Bureau de Recherches Géologiques et Minières, BP 6009 45060 Orléans Cedex 2, France
[4]EDF – Recherche et Développement, Laboratoire National d'Hydraulique et Environnement, Chatou, France

Correspondence: Hanieh Seyedhashemi (hanieh.seyedhashemi@inrae.fr)

Abstract.

Stream temperature appears to be increasing globally, but its rate remains poorly constrained due to a paucity of long-term data and difficulty in parsing effects of hydroclimate and landscape variability. Here, we address these issues using the physically-based thermal model T-NET (Temperature-NETwork) coupled with the EROS semi-distributed hydrological model to reconstruct past daily stream temperature and streamflow at the scale of the entire Loire River basin in France ($10^5 \, \mathrm{km}^2$ with 52 278 reaches). Stream temperature increased for almost all reaches in all seasons (mean = +0.38 °C/decade) over the 1963–2019 period. Increases were greatest in spring and summer with a median increase of +0.38 °C (range=+0.11 ~~–~~to +0.76 °C) and +0.44 °C (+0.08 ~~–~~to +1.02 °C) per decade, respectively. Rates of stream temperature increases were greater than for air temperature across seasons for ~~50–86 %~~ majority of reaches. Spring and summer increases were typically the greatest in the southern ~~headwaters~~ part of the Loire basin (up to +1 °C/decade) and in the largest rivers (Strahler order ≥ 5). Importantly, air temperature and streamflow ~~exerted~~ could exert joint influence on stream temperature trends, where the greatest stream temperature increases were accompanied by similar trends in air temperature (up to +0.71 °C/decade) and the greatest decreases in streamflow (up to -16 %/decade). Indeed, for the majority of reaches, positive stream temperature anomalies exhibited synchrony with positive anomalies in air temperature and negative anomalies in streamflow, highlighting the dual control exerted by these hydroclimatic drivers. Moreover, spring and summer stream temperature, air temperature, and streamflow time series exhibited common change-points occurring in the late 1980s, suggesting a temporal coherence between changes in the hydroclimatic drivers and a rapid stream temperature response. Critically, riparian vegetation shading mitigated stream temperature increases by up to 16 % in smaller streams (i.e. <30 km from the source). Our results provide strong support for basin-wide increases in stream temperature due to joint effects of rising air temperature and reduced streamflow. We suggest that some of these climate change-induced effects can be mitigated through the restoration and maintenance of riparian forests~~, and call for continued high-resolution monitoring of stream temperature at large scales.~~.

1 Introduction

Stream temperature is a critical water quality parameter affecting the distribution of aquatic communities (Poole and Berman, 2001; Ducharne, 2008), but its future under global change remains uncertain. As air temperature (Ta) increases worldwide due to climate change, stream temperature (Tw) is expected to follow a similar trajectory (Mohseni et al., 1999; Kaushal et al., 2010; Van Vliet et al., 2011; Isaak et al., 2012; Arora et al., 2016). Indeed, there is growing evidence that stream warming is occurring around the world, affecting freshwater ecosystems through structural and functional changes in biological communities throughout the food web (Woodward et al., 2010; O'Gorman et al., 2012; Scheffers et al., 2016). Deleterious warming effects are documented from bottom-dwelling microorganisms (e.g. Romaní et al., 2016; Majdi et al., 2020) up to macroinvertebrates (e.g. Floury et al., 2013; Bruno et al., 2019) and fish communities (e.g. Maire et al., 2019; Stefani et al., 2020). However, the paucity of long-term time series of Tw (Webb and Walling, 1996; Nelson and Palmer, 2007; Webb et al., 2008; Arora et al., 2016) has impaired the larger scale assessment of such trends, especially in light of confounding factors like hydrological changes and land use change. Hence, analyses of Tw trends, especially at large spatiotemporal scales, remain scarce (but see Kaushal et al., 2010; Orr et al., 2015; Arora et al., 2016; Michel et al., 2020; Wilby and Johnson, 2020).

To overcome the lack of Tw data, large-scale ecological studies typically use Ta as a proxy for Tw to assess the impact of climate change on the spatial distribution of aquatic organisms (e.g. Buisson et al., 2008; Buisson and Grenouillet, 2009; Tisseuil et al., 2012; Domisch et al., 2013), but Ta can over-predict changes to stream fish assemblages with climate warming compared with Tw (Kirk and Rahel, 2022). Indeed, Ta can be an imprecise surrogate for Tw (Caissie, 2006) . Indeed, since many landscape and basin characteristics (e.g. stream discharge Q(Q), streambed morphology, karst resurgences, topography, and vegetation cover) contribute to the response of Tw to climate change over time and space (Stefan and Preud'homme, 1993; Webb and Walling, 1996; Webb et al., 2008; Hannah and Garner, 2015). For instance, riparian vegetation can obstruct solar radiation, which is the dominant heat flux at air-water surface (Hannah et al., 2004; Caissie, 2006), and therefore decrease Tw response to Ta (Johnson, 2004; Loicq et al., 2018). However, while riparian vegetation shading can greatly decrease the temperature of small rivers (Dan Moore et al., 2005; Loicq et al., 2018), it has limited effects on larger rivers since the width of such rivers is large enough that only a small part of it can be shaded. Rising groundwater temperature (Taylor and Stefan, 2009; Kurylyk et al., 2013, 2014) and reduced groundwater flows (Kurylyk et al., 2014) due to climate change may further contribute to Tw trends (Meisner, 1990; Arora et al., 2016), leading to asymmetric controls (vis-à-vis Ta) on Tw (Moatar and Gailhard, 2006), especially in headwaters (Caissie, 2006; Kelleher et al., 2012; Mayer, 2012). Finally, intensification of the water cycle (Huntington, 2006), with more frequent and severe droughts (Mantua et al., 2010; Giuntoli et al., 2013; Prudhomme et al., 2014), as well as more intense and sudden floods (Blöschl et al., 2019) may decouple Ta-Tw trends, exacerbating Tw increases that will most likely be evident during low summer flows when thermal capacity inertia and flow velocity are at their minima (Webb, 1996; Webb et al., 2008).

There is thus a clear need to improve our estimates of Tw trends to assess how stream ecosystems will respond in the face of a changing climate to the climate change. Unfortunately, extrapolating trend estimates derived from short time series may lead to paradoxical results, e.g. cooling streams in a warming world (Arismendi et al., 2012). This discrepancy in short-

and long-term dynamics is likely due to confounding influences of Ta and hydrology, with implications for the persistence of specialized aquatic organisms (e.g., for cold-water biota, Arismendi et al., 2013b) and the completion of their life cycle (e.g., for diadromous fish, Arevalo et al., 2020). Hence from an ecological perspective, it will be critical to understand and deconvolve the joint influences of changing Tw and Q regimes. In the absence of more robust data sources, modeling is thus an indispensable tool in meeting the these goals.

Tw models output data sets that can then be used to assess the magnitude of long-term trends, but model selection entails important considerations. For example, Tw can be estimated by developing a statistical, or stochastic, model based on multiple independent drivers (Benyahya et al., 2007), which is a common practice for large scale studies (e.g. Mantua et al., 2010; Jackson et al., 2017, 2018). However, these statistical models lack mechanism; they cannot reveal the specific energy transfer mechanisms responsible for the spatiotemporal patterns of Tw (Dugdale et al., 2017). They are also unable to predict Tw for periods other than those used for their calibration due to, for instance, the non-stationary relationship between Ta and Tw over time (Arismendi et al., 2014). Alternatively, physically-based, or deterministic, models are entirely mechanistic; they predict Tw dynamics through a heat budget, accounting for energy exchanges and effects of landscape characteristics on energy transfer (Sinokrot et al., 1995; Webb and Walling, 1997; Yearsley, 2009; ?)(Sinokrot et al., 1995; Webb and Walling, 1997; Yearsley, 2009; van V. Critically, such process-based models can be used not only to reconstruct past time series, but they can be used in forecasting, or in predicting Tw response to projected climate or land-use changes (Caissie et al., 2007; Dugdale et al., 2017).

Here, we used a physical process-based thermal model coupled with a semi-distributed hydrological model to understand how Tw has responded to recent climate change at a large scale. To do so, we first assessed the performance of the models against field observations over the Loire basin, France, then reconstructed daily Q and Tw over the past 57 years over the whole hydrographic network. We then used model outputs reconstructed time series to compute the magnitude of decadal trends in seasonal and annual Tw, Ta and Q. To understand the relative influences of Q and Ta Ta and Q (as the main hydroclimate drivers of Tw) on Tw, we compared their trends, anomaly behaviors, and temporal patterns and assessed their spatial and temporal links. Finally, we sought to understand variation in Tw trends as a function of stream size, landscape attributes, and riparian shading.

2 Study area

The Loire River basin is one of the largest in Europe ($10^5 \, \text{km}^2$) encompassing an area with starkly contrasting HydroEco Regions ("HER"), land use/land cover, and climatic conditions (Moatar and Dupont, 2016), providing an ideal case study to disentangle the drivers of the spatial heterogeneity of trends in Tw. Mean annual precipitation (549–2130 mm), mean annual potential evapotranpiration (PET) (550–850 mm), mean annual Ta (6.0–12.5 °C) (see Fig. S1), and altitude (0–1850 m) (see Fig. 1, right) provide spatially variable controls on stream thermal regimes. There are three main HER in this basin (Wasson et al. (2002) identified several Hydro-Ecoregions (HER) over France, representing homogeneous areas in terms of land use/land cover, geology, and climate conditions. A grouping over the Loire basin was done to identify three contrasted HERs (identified as A, B, and C in Fig. 1, middle) , which were categorized based on climate, lithology, and relief (Wasson et al., 2002)) that can be used to describe the spatial heterogeneity in Tw at the basin scale. Granite and basalt dominate the southern headwaters of

the basin (mostly in the Massif Central, HER A), whereas sedimentary rocks occupy the middle reaches with a potential for
groundwater input (HER B), followed by granite and schist in the lower reaches (HER C) (see Fig. 1, ~~top).~~ left). The percentage of riparian vegetation cover (mean over both sides of a river bank at a buffer of 10 m, Valette et al., 2012) is more important in HER A (median=73%) and in HER B (median=68%) (Fig. 1, middle). In HER C, the presence of riparian vegetation is quite heterogeneous (median=50%).
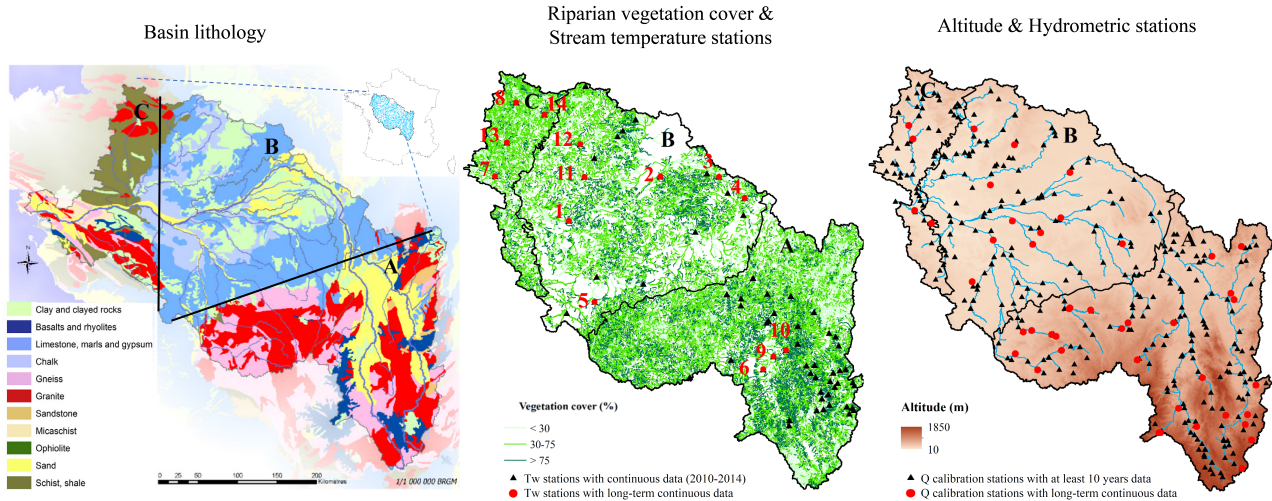
Figure 1. Maps of the Loire basin. ~~(top) Main aquifer formations and lithology, (middle) riparian vegetation cover (Valette et al., 2012) and Tw stations, and (bottom) altitude (IGN, 2011) and hydrometric stations. The lithology map was~~ Left panel: basin lighology adapted from Moatar and Dupont (2016), based on original data from BRGM (French Geological Survey). The figure in the top right corner of left panel shows the position of the Loire River basin in France. Middle panel: riparian vegetation cover (provided by Valette et al., 2012) and Tw stations. All Tw stations were used to assess the performance of the T-NET thermal model (see Table S5), but only the ones with long-term data (in red) were used to assess the T-NET thermal model accuracy for long-term trends. Complete information on Tw stations with long-term continuous data are provided in Table 1. The numbers in red in the middle panel correspond to the ID of long-term Tw stations in Table 1. Right panel: altitude (IGN, 2011) and hydrometric stations (extracted from French national Banque Hydro database: http://www.hydro.eaufrance.fr/). All hydrometric stations were used for calibrating the EROS hydrological model (see Table S2), but only stations on the French Reference Hydrometric Network (RHN) with long-term data (in red) were used to assess the EROS hydrological model performance on long-term trends (see Table S4).

3 Method and data

We assessed how Tw responded to climate change over the past 57 years in the Loire River basin in four steps. First, we applied physically based Q and Tw models for the period 1963–2019. Second, we assessed ~~model~~ both hydrological and thermal models performance by comparing simulated ~~daily~~ seasonal and annual Q and Tw to data from observation stations. Third, we

assessed Q and Tw long-term trends. Fourth, we analyzed how hydro-climatic changes and landscape features could explain reconstructed trends in Tw. We performed all analyses on both seasonal and annual basis, where winter is December-February

100 (DJF), spring is March-May (MAM), summer is June-August (JJA), and fall is September-November (SON). Analyses were also performed by HER (see Fig. 1, and section 2) to look at the large-scale influence of lanscape characteristics.

3.1 Modeling daily Q and Tw

We used two models to calculate Tw in the Loire River basin according to the method developed by Beaufort et al. (2016). The first model is the EROS semi-distributed hydrologic model, which estimates daily Q at sub-basin outlets. The second model is

105 the fully distributed, mechanistic temperature model called Temperature-NETwork (T-NET; Beaufort et al., 2016; Loicq et al., 2018) that uses Q from EROS and meteorological reanalysis data from Safran atmospheric reanalysis data (Quintana-Segui et al., 2008; Vidal et al to estimate Tw at each reach in the Loire River basin. These models are briefly described below, and are detailed in Thiéry (1988); Thiéry and for EROS, and Beaufort et al. (2016); Loicq et al. (2018) for T-NET.

3.1.1 EROS hydrological model principles and input data

110 The EROS ~~hydrological model uses daily~~ semi-distributed hydrological model simulates daily Q at the outlet of 368 sub-basins (ranges between 40 and 1600 km^2; mean drainage area = 300 km^2), designed to be as homogeneous as possible with respect to land use and geology. On each of these sub-basins, the water balance is modelled by a lumped model using three reservoirs (see Fig. S2) and a routing function for propagation across sub-basins (Thiéry, 1988; Thiéry and Moutzopoulos, 1995; Thiéry, 2018) . Water abstractions are not considered in EROS, and it produces natural Q. This hydrological model has already been used in

115 several other studies including climate change impact studies (Ducharne et al., 2011; Habets et al., 2013; Bustillo et al., 2014) .

EROS used daily Ta (°C), solid and liquid precipitation (mm), and reference evapotranspiration (ET_0, mm) to produce mean daily Q and groundwater flows (Thiéry, 1988; Thiéry and Moutzopoulos, 1995; Thiéry, 2018). Meteorological inputs were provided by the 8 km gridded Safran atmospheric reanalysis data released by Meteo-France over the 1958–2019 period

120 (Quintana-Segui et al., 2008; Vidal et al., 2010). ET_0 was computed from Safran variables with the Penman-Monteith equation (Allen et al., 1998). ~~Observed Q data were extracted form the French national Banque Hydro database () for all available stations across the Loire basin (Fig. 1, bottom). Stations along the main Loire and Allier rivers were highly influenced by the management of large dams, notably through summer releases to sustain low-flows. Time series at these stations have been first naturalized by EDF (French Electricity) by taking into account recorded dam storages and releases. EROS was calibrated~~

125 ~~over the 1971–2018 period against daily Q at 352 sub-catchments (range=40-1600 , mean=300) with at least 10 years of daily observations (Fig. 1). The calibration aimed at maximizing the Nash-Sutcliffe efficiency criteria (Nash and Sutcliffe, 1970) on the square root of streamflow and minimizing the overall bias, in order to simulate correctly the whole range of Q values (Thiéry, 1988; Thiéry and Moutzopoulos, 1995; Thiéry, 2018). A 3-year warm-up period (1971–1974) was discarded from the calibration period (1971–2018, which maximizes the amount of streamflow observations). The calibrated model was then used~~

130 ~~to simulate streamflow over 368 sub-catchments in the Loire basin over the whole 1963–2019 period. Streamflow was then~~

distributed along the river network according to the drainage area for informing the T-NET model at the reach scale. Although meteorological variables were available from 1958, the first three years (1958-1962) was discarded for the sake of model convergence.

3.1.2 T-NET thermal model principles and input data

135 The T-NET (Temperature-NETwork) thermal model computes Tw along the longitudinal dimension of the hydrographic network (a GIS polyline) of the Loire River basin. To simulate Tw, the equilibrium temperature (Te) is first computed,the temperature at which the net heat flux across the surfaces of the stream is null (Bustillo et al., 2014)is a fully mechanistic, 1D model that simulates hourly $Tw_{i,j}$ at distance, i, along reach, j, by solving the local heat budget. The heat budget of each reach includes six fluxes ($W.m^{-2}$): net solar radiation, atmospheric longwave radiation, longwave radiation emitted from the

140 water surface surface water, evaporative heat flux, convective heat flux, and groundwater heat inflow. flux. Briefly, the model calculates the longitudinal change in Tw at time t (dTw/dx) for steady-state conditions in order to achieve thermal equilibrium (i.e. $\Sigma H_{i,j} = 0$, where H is a heat flux), while accounting for confluence mixing. Detailed information about the T-NET model principles and calculation of the six heat fluxes at the water-air and water-stream bed interfaces, and thermal propagation were provided in Beaufort et al. (2016) and Loicq et al. (2018).

145 The hydrographic network of the model over the Loire basin consists of 52 278 reaches delimited either by confluences of two streams or a headwater source (i.e. first order reaches) (Beaufort et al., 2016; Loicq et al., 2018). The mean reach length is 1.7 km and 74 % of the reaches have a Strahler order lower than 3. 3 (see Fig. S3). To compute the six heat fluxes and the water travel time for each reach, the following input data were used:

- Meteorological variables: hourly Ta (°C), specific humidity ($g.kg^{-1}$), wind velocity ($m.s^{-1}$), shortwave radiation ($W.m^{-2}$)
150 and longwave radiation ($W.m^{-2}$) were provided by the 8 km gridded Safran atmospheric reanalysis (Vidal et al., 2010). All reaches within a grid cell were assigned the values of the meteorological variables in that grid cell. For reaches flowing through more than one grid cell, meteorological variables were weighted by the relative length of the reach within each grid cell.

- Riparian vegetation shading: riparian vegetation is one of the major regulators of shortwave radiation. In the current
155 study, patches of wooded area provided by the BD TOPO® (IGN, 2008) database were used as a proxy of vegetation. The vegetation species and length of each wooded patch in a buffer of 10 m were extracted for both right and left river banks (van Looy and Tormos, 2013). The vegetation density (vc) was then calculated as the ratio of patch length to reach length for both right and left river banks. In case of multiple wooded patches in any side of a river bank, the average vegetation density of the patches was considered. Then, the model proposed by Li et al. (2012) was used for the
160 calculation of the dynamic shading factor (SF) at hourly time step. The required average tree height for both right and left river banks was estimated based on vegetation species (see Table S1).

In the presence of different vegetation species, the average tree height (m) for each side of a river bank was calculated as follows:

$$H = \frac{1}{n}\Sigma_{i=1}^{n} H_i \frac{L_i}{L} \tag{1}$$

 with H_i and L_i the height and length of the tree patch i, respectively, and L the reach length. Next we calculated the proportion of the river width that was shaded (W_{shaded}) and the dynamic shading factor (SF) as follows:

$$W_{\text{shaded}}(t) = \frac{H_{\text{left/right}} \times \cot \Psi \times \sin \delta}{W} \; \frac{H_{\text{left/right}} \times \cot \Psi(t) \times \sin \delta(t)}{W(t)} \tag{2}$$

$$SF_{\text{right}}(t) = (W_{\text{shaded}})_{\text{right}}(t) \times (vc)_{\text{right}} \tag{3}$$

$$SF_{\text{left}}(t) = (W_{\text{shaded}})_{\text{left}}(t) \times (vc)_{\text{left}} \tag{4}$$

$$SF(t) = Max(SF_{\text{right}}(t), SF_{\text{left}}(t)) \tag{5}$$

where H is the average tree height (see Eq. 1), W is the river width (see Eq. ??7), Ψ is the solar altitude angle, δ is the angle between solar azimuth and the mean azimuth of T-NET reach, and vc is the vegetation density. Loicq et al. (2018) already tested this method and showed that Tw simulated by the above method was close to observed Tw. To take into account the phenology and stages of leaf growth, a coefficient corresponding to each season and transmissivity was applied to SF to calculate the final shading factor: $SF_{final} = SF \times (1 - transmissivity)$. The transmissivity in leafless months (Jan, Feb, Nov and Dec), months of leaf growth (Mar and Apr), and full-leaf months (May-Sep) was fixed to 0.3, 0.2 and 0, respectively, following Hutchison and Matt (1977). The shortwave radiation was lastly regulated by a factor of $1 - SF_{final}$.

- Reach streamflow: the daily Q simulated at the outlet of 368 homogeneous sub-basins by the EROS model (see section 3.1.1) were redistributed along the river network inside each sub-basin according to the reach drainage area for informing the T-NET model at the reach scale. The ratio of sum of the lengths of all reaches upstream of a reach to the sum of the lengths of all reaches located in a sub-basin was used as a proxy for the drainage area of a reach. To have Q at hourly time step, Q was assumed to be constant over 24 hours.

- River hydraulic geometry: stream depth and width were calculated using a hydraulic model assuming a rectangular river section being constant over 24 hours (Morel et al., 2020):

$$D(t) = D50 \times \left[\frac{Q(t)}{Q50}\right]^f \tag{6}$$

$$W(t) = W50 \times \left[\frac{Q(t)}{Q50}\right]^b \tag{7}$$

with f and b being at-a-reach exponents previously predicted by climate, hydrological, topographic and land use descriptors (see Morel et al., 2020, for more details). $Q(t)$ is the daily mean streamflow provided by the EROS hydrological

model. The Q50, W50, D50 (the median of Q, width and height, respectively) and the exponents were available on the Theoretical Hydrographic Network for France (RHT, Pella et al., 2012). There was about 50 % correspondence between the reaches of the T-NET and RHT networks. For the rest of them, required hydraulic geometry variables for the T-NET reaches were extrapolated from the nearest RHT reach. These river hydraulic geometries allowed us to calculate the water velocity by the ratio of $Q(t)$ to rectangular wetted cross-section. The travel time was also defined by the ratio of water velocity to reach length.

3.2 Model assessment and validation

3.2.1 Calibration and assessment of EROS hydrological model

For calibration, 352 hydrometric stations with observed Q data (see Table S2) extracted from the French national Banque Hydro database (http://www.hydro.eaufrance.fr/), were used (Fig. 1, right). Stations along the main Loire (14 stations) and Allier (11 stations) rivers were influenced by operations of 4 large dams for hydropower, flood control and low-flow management, notably through summer releases (see Table S3). Time series at these stations have been first naturalized by EDF (Électricité de France) based on variations in water storage in reservoirs due to operations based on target storage curves (Naussac, Villerest) and optimization of the hydropower energy generation for the electric grid needs (Grangent, Montpezat). EROS was then calibrated over the 1971–2018 period (which maximizes the number of available streamflow observations) against daily Q at all 352 sub-basins with at least 10 years of daily observations. Note that in the current study, calibrating EROS by performing a classical split-sample test was not possible due to the numerous and diverse gaps in streamflow observations at this large scale. Therefore, calibration was done on the complete set of available information over the past decades which is a standard approach for calibrating a hydrological model in climate change impact studies (e.g. Habets et al., 2013; Vidal et al., 2016).

The calibration aimed at optimizing all unknown parameters (soil capacity, recession times, and propagation times) through maximizing the Nash-Sutcliffe Efficiency (NSE) criterion on the square root of streamflow and minimizing the overall bias. Considering the NSE criterion on the square root of the flows provided an estimate of model performance without favoring neither high flows nor low flows. The overall calibration criterion, C, was: C = mNSE – w.mRB where mNSE is the mean NSE, mRB is mean relative bias, and w is a weighting factor fixed at 0.05. A 3-year warm-up period (1971–1974) was discarded from the overall calibration period for the next assessments.

The calibrated model was then used to simulate streamflow over the whole 368 homogenous sub-basins in the Loire basin over the whole 1963–2019 period. Note that although meteorological variables were available from 1958 onwards, the first years (1958-1962) were discarded from the analysis to ensure the EROS model convergence.

Of the 352 calibration stations considered by EROS, 44 ~~are~~ were part of the French Reference Hydrometric Network (RHN) described by Giuntoli et al. (2013) with long-term continuous high-quality data over the 1968–2019 period, especially for low-flows (see Table S4). These stations are shown with red points in Fig. 1, right. Seasonal and annual relative biases, together with Nash-Sutcliffe efficiency on Q, $ln(Q)$, and $\sqrt{Q}$ were computed ~~over the 1968–2019 periodon these RHN stations~~ on both 352 calibration (over the 1975–2018 period) and 44 RHN stations (over the 1968–2019 period) to provide an overview

of the performance of the EROS model. Moreover, to asses EROS model ability to capture long-term trends, decadal trends (in % per decade) over the 1963–2019 period on seasonal and annual averages from the EROS simulation were compared to corresponding observed trends at each of the 44 ~~reference stations~~ RHN stations with long-term continuous daily data.

3.2.2 Validation of T-NET thermal model

3.2.3 ~~T-NET thermal model~~

~~The~~ T-NET ~~model~~ does not consider the influence of impoundments on thermal energy balance, and thus produces ~~"~~"natural" thermal regimes. Therefore, model performance was assessed on ~~natural~~ near-natural Tw stations, which are also weakly influenced by impoundments ~~.~~ i.e. at 67 ~~near-natural~~ stations with continuous daily data over the 2010–2014 period (see Fig. 1~~)~~, middle, and Table S5). These stations were identified using the thermal signatures approach that allows distinguishing between natural and altered thermal regimes (see Seyedhashemi et al., 2020, for more details). Of these identified natural ~~reaches, 58~~ stations, 55 were located on small/medium streams (with distance from the source $<100\,\mathrm{km}$), while the remaining ~~are~~ were located on large rivers. The mean catchment area of natural stations was $151\,\mathrm{km}^2$ (± 225~~range=7-1342~~ km^2) for small/medium streams, and $18\,926\,\mathrm{km}^2$ ($\pm 18{,}833$~~range=1931-57\,043~~ km^2) for large rivers. Tw data at these 67 stations were provided by different organizations: EDF (Électricité de France), OFB (Office français de la biodiversité), and DREAL (Direction régionale de l'environnement, de l'aménagement et du logement), and FD (Fédération Nationale de la Pêche) (see Tables 1 and S5). Tw data provided by OFB can be downloaded from http://www.naiades.eaufrance.fr/. The rest of Tw data are not archived for the public use. Seasonal and annual absolute biases, and Root mean square error (RMSE) were assessed at these 67 stations. Note that unlike the EROS hydrological model, the T-NET thermal model does not have any free parameter, hence, it did not require calibration.

Long-term continuous data was available at 14 of the 67 near-natural stations, including 9 stations with 8-13 years data and 5 stations with 20-40 years data. These 14 stations are represented as red points in Fig. 1, middle~~)~~, and listed in Table 1. The long-term evolution of annual mean Tw at these stations ~~is~~ was shown in Fig. ~~S1~~S4. These 14 near-natural stations with long-term continuous data ~~comprise~~ comprised the validation dataset for the seasonal and annual trend assessment (see Table 1).

3.3 Time series reconstruction and assessment of long-term trends

Daily Q and Tw were reconstructed over the 57-yr period 1963–2019 using the EROS hydrological model and the T-NET thermal model. For each of the 52 278 ~~river~~ reaches, daily time series of Ta (from the Safran reanalysis), Q (from EROS), and Tw (from T-NET) were reconstructed. Seasonal and annual averages of these ~~3~~ three variables were considered in the trend assessment. Map of annual mean Tw, Ta and Q over the 1963–2019 period were presented in Fig. S5 with annual $\mathrm{Tw} > 11.5\,^{\circ}\mathrm{C}$ for large rivers (annual $\mathrm{Ta} > 10.5\,^{\circ}\mathrm{C}$ and $\log(\text{annual } \mathrm{Q}) > 1\,\mathrm{m}^3/\mathrm{s}$).

We estimated the magnitude of trends in these time series with the non-parametric Theil–Sen estimator (Sen, 1968), and evaluated their significance with the Mann-Kendall test (Mann, 1945), commonly used in hydrological analyses (see e.g. Giuntoli et al., 2013) but also thermal analyses (e.g. Kaushal et al., 2010; Arismendi et al., 2013a; Arevalo et al., 2020).

255 This test is robust to non-normal data, non-linear trends, and series with outliers and missing values. Trend magnitudes ~~are~~ were reported in °C/decade for Ta and Tw, and in %/decade for Q (percentage of changes over whole period) ~~,~~ to help for comparisons across the basin.

3.4 Hydroclimatic drivers of Tw trends

~~Distributions of trends~~ Many factors affect the spatio-temporal variability of Tw. In the current study, we considered Ta
260 as a proxy for heat fluxes and meteorological variables, and Q as a proxy for thermal inertia and hydraulic geometries (which depends on Q, see Eq. 6 and 7). To understand variability in Tw trends, we assessed spatial coherence and temporal synchronicity between trends in Tw and ~~Ta~~ trends in Ta and Q as the main hydroclimate drivers influencing Tw. To do so, we first assessed the spatial coherence between these variables. In this regard, distributions of trends in Tw and Ta were first compared for the whole basin at the seasonal and annual scales using the non-parametric Wilcoxon signed rank test (Bauer,
265 1972) to determine whether median Tw trends were greater than median Ta trends. ~~To assess how Ta and Q influenced Tw, we first identified which reaches exhibited 1) jointly increasing trends in~~ Then, the spatial coherence across reaches in terms of difference in trends between Tw and Ta ~~, and 2) jointly increasing trends in~~ on one hand, and sign of trend in Q on the other hand, was assessed to explain the discrepancy between Tw and Ta ~~and decreasing trends in Q. Then,~~ found in the previous step with respect to Q.

270   Then, we assessed the temporal link between these three variables (i.e. Tw, Ta and Q). To do so, for each identified reach, we first evaluated the strength and direction of ~~these~~ joint trends using Pearson correlation between ~~1~~i) Tw and Ta, and ~~2~~ii) Tw and ~~log(Q).~~

   Q. Ta, Tw, and Q seasonal and annual anomalies – with respect to the 1963–2019 interannual mean – were then used to assess the synchronicity of extreme years and change-point in time series. Change-points in time series of anomalies at each
275 reach were computed with the non-parametric Pettitt test that considers no change in the central tendency as a null hypothesis (Pettitt, 1979). Change points were reported at the 95 % confidence level.

3.5 Landscape drivers of Tw trends

Stream size ~~and HER (see Fig. 1) were~~ , within individual large-scale homogeneous HERs, was selected as the first major potential landscape ~~drivers~~ driver. The Strahler order of each reach was used as a proxy for stream size. Reaches with Strahler
280 order 5–8 were combined into a single group termed "large rivers". The Spearman correlation was computed between ~~median~~ decadal trends in Tw (i.e. ~~median~~ across all reaches) and Strahler order. Such correlations were computed across HERs and at seasonal and annual scales to evaluate the spatial heterogeneity and seasonality. Finally, in order to better illustrate the relationship between trends in Tw and Strahler order, median Tw trends of each group of rivers with respect to Strahler order was presented.
285   ~~Lastly~~Second, the influence of riparian vegetation shading on trends in Tw was assessed using the daily average of the riparian vegetation shading (SF) simulated by T-NET. Seasonal shading was computed as the average of the daily SF over each season. For this analysis, only low-order reaches – distance from the source $< 30\,\mathrm{km}$ – were considered, based on previous

observations that riparian shading primarily influences Tw at this scale (Dan Moore et al., 2005; Loicq et al., 2018). Then, as for the previous analysis for the influence of stream size, the correlation between ~~median~~ decadal Tw trends and five levels

290 of riparian shading (<15 %; 15-25 %; 25-40 %; 40-60 %; >60 %) was computed across HERs and seasons. Finally, median Tw trends were compared for each level of riparian shading.

4 Results

4.1 Performance of models against observations

The EROS model performed well at the 352 calibration stations at the annual scale with a median relative bias close to 0%

295 (see Fig. S6, left). It slightly underestimated winter Q (median relative bias (across stations)=-6.27%) and spring Q (-3.47%), and overestimated summer Q (+34.7%) and fall Q (+20.9%). The EROS model also performed well at 44 RHN stations with long-term continuous daily data at the annual scale with a median relative bias of 0.37% (see Fig. ~~S2~~S6, right). It slightly underestimated winter Q (median ~~bias~~relative bias (across stations)=-7.26%) and spring Q (-6.79%), and overestimated summer Q (+37.7%) and fall Q (+24.7%). The mean NSE criteria for ~~low, mean and high flows were 0.82, 0.85 and 0.79, respectively.~~Q,

300 $ln(Q)$, and $\sqrt{Q}$ was > 0.7 for at least 75 % of both calibration and RHN stations (see Fig. S7). A good performance of the EROS model in reconstructing daily Q was also seen at three different hydrometric stations located in the upstream, the middle, and the downstream part of the Loire River basin (see Fig. S8).

No systematic bias was ~~observed for modeled Tw~~ found for Tw modeled by T-NET at the stations located on small and medium rivers (see Fig. ~~S2~~S9, top left). Median Tw bias ranged from -0.26 °C (in fall) to 0.8 °C (in winter). Large rivers

305 exhibited a small Tw underestimation ~~,~~(see Fig. S9, top right), with a median bias ranging from -0.29 °C (in fall) to +0.15 °C (in winter), and the overall biases were still quite small across seasons (~~IQR~~Interquartile Range (IQR)=0.4–0.7 °C ~~).~~depending on season). On the other hand, the median RMSE of the T-NET thermal model, for small and medium rivers, ranged between 0.52 °C (in annual) and 0.91 °C (in DJF and JJA) across seasons (see Fig. S9, bottom left). For large rivers, the median RMSE of the T-NET thermal model ranged between 0.38 °C (annual) and 1.11 °C (SON) across seasons (see Fig. S9, bottom right).

310 Moreover, 53-83% stations (resp. 50-100%) on small and medium (resp. large) rivers had a RMSE < 1 °C across seasons.

Trends in observed and modeled Q were ~~well~~significantly correlated for all seasons (Fig. ~~S3~~S10), with the highest correlation across stations found in spring (~~r = 0.69, p < 0.05~~and fall (r=0.69 and 0.71, p < 0.05) and the lowest correlation found in summer~~(r = 0.17, p = 0.26). Both~~, which was also non-significant (r=0.17, p=0.26). The trends of both modeled and observed Q were slightly decreasing (up to -11 ~~%/decade~~) for the majority of stations across all seasons, but the trend was significant

315 for a very few of them (and mostly at the annual scale), all located in the southern ~~headwaters~~ part of the basin in HER A (red points of Fig. ~~S3~~S10). Moreover, there were only a few discrepancies between estimates of trend significance in modeled and observed Q across seasons (11-18 % of stations).

Modeled and observed Tw trends ~~correlated well~~ also correlated significantly (see Fig. ~~S4~~S11) across seasons, with the highest correlation in summer (~~r = 0.94, p < 0.05~~r=0.94, p < 0.001) and the lowest correlation in fall~~(r = 0.29, p = 0.32).~~

320 , which was also non-significant (r=0.29, p=0.32). There was also good agreement between estimates of trend significance

in modeled and observed Tw across seasons. Indeed, the trends in observed and simulated Tw were either both significant or neither was significant. Contrasting with trends in Q, trends for Tw increased for most stations across seasons, but the short period of record led to mostly non-significant ~~(p=0.05)~~ trends. However, stations with long-term data showed significant increasing trends for all seasons, with the exception of winter (Fig. ~~S4~~S11). A visual comparison of observed and modeled
Tw time series and trends at stations with long-term data (> 20 years) indeed suggested a strong coherence and agreement between observations and simulations provided by T-NET for all seasons (Fig. 2). For the four stations along the main stem of the Loire ~~river (Fig~~River (Fig. 2), the greatest increase occurred in spring – +0.61 (resp. +0.71) °C/decade in observations (resp. simulations) – and summer – +0.62 (resp. +0.58) °C/decade in observations (resp. simulations). The smallest increase was found in winter – +0.22 (resp. +0.28) °C/decade in observations (resp. simulations).

4.2 Spatial reconstruction of long-term trends

Tw significantly increased in almost all modeled reaches for all seasons (Fig. 3, left~~;~~, and Fig. ~~S5~~S12, left). Depending on the season considered, 62 % to 80 % of reaches showed trends in the range of +0.2 ~~–~~to +0.4 °C/decade (i.e. +1.14 ~~-2.28~~to +2.28 °C over the whole 1963–2019 period, see Fig. S13). Summer Tw trends were more spatially variable than in other seasons, with more than 50 % of reaches showing values higher than +0.4 °C/decade (see Fig. ~~S6~~S13). Such reaches were mainly located in the southern part of the basin, in HER A (see Fig. 3, left). Spring Tw trends showed a similar spatial pattern, but with lower trend values.

Likewise, Ta exhibited increasing trends for 99 % of all reaches across spring, summer, and the whole year (~~Fig~~Figs. 3, middle and S12, middle). Values were mainly in the range of +0.2 ~~–~~to +0.4 °C/decade (see Fig. ~~S6~~S13). The highest Ta trend values were found in summer ~~(resp. spring)~~and spring, when 67 % ~~(resp.~~and 22 % ~~) of reaches~~of reaches, respectively, showed values higher than +0.4 °C/decade. Such reaches were mainly located in HER A~~, especially in summer~~. Non-significant trends were found over the whole basin in winter, and in the southern part of the basin in fall.

In contrast to Ta and Tw, trends in Q were highly variable in magnitude and direction across the basin and across seasons (Fig. 3, right), and most were not significant at p=0.05 (Fig. ~~S5~~S12, right). However, significant decreasing trends were found in the southern ~~headwaters~~part of the basin (HER A) in spring, summer, fall, and ~~annual~~at annual time scale (Fig. ~~S5~~S12). Decreasing trends were observed for ~~the~~a majority of reaches across seasons (66-83% of reaches), with the exception of winter (37%) ~~.~~(see Fig. S14). Decreasing trends could have magnitudes greater than -5 % per decade, implying a -28 % loss in Q over the whole 1963–2019 period ~~.~~(see Fig. S14).

4.3 Hydroclimatic drivers of Tw trends

~~Relationships between trend estimates~~Spatial coherence

The ~~median~~medians of Tw trends were higher than ~~that~~those of Ta trends for every season (p<0.001 according to the Wilcoxon signed rank test), except for summer when the median trend values for Tw and Ta were very similar, but more variable for
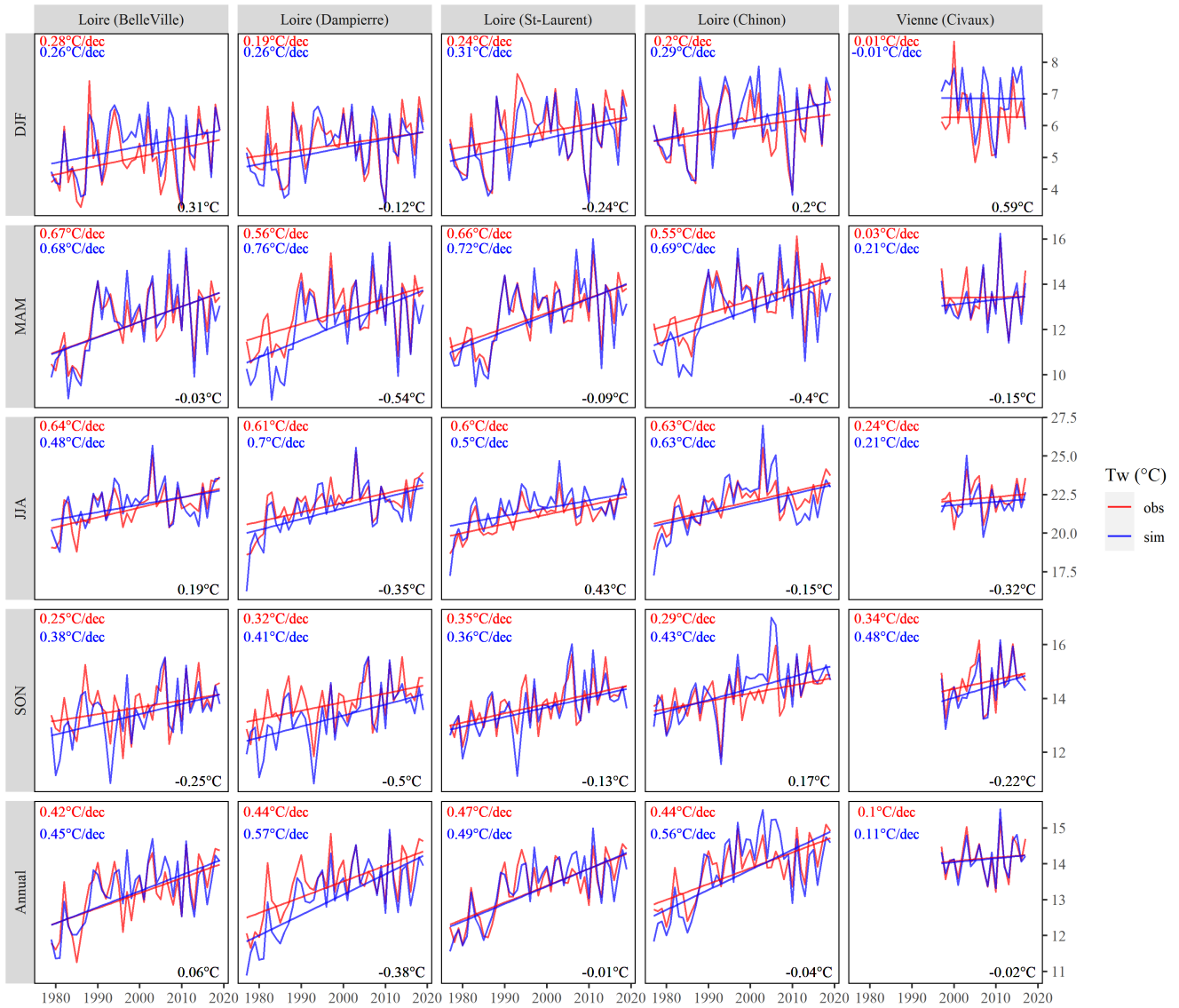
Figure 2. Seasonal and annual time series of observed and simulated Tw at stations with at least 20 years long-term continuous data between 1977 and 2019 (see Table 1 for more information)between 1977 . The red and 2019. blue solid lines show trend in observed and simulated Tw. Numbers in red and blue in the top left corner of each graph show trend values magnitudes (Sen's slope) in observed and simulated Tw. Numbers in black in the bottom right corner of each graph show the mean bias of the reconstruction.
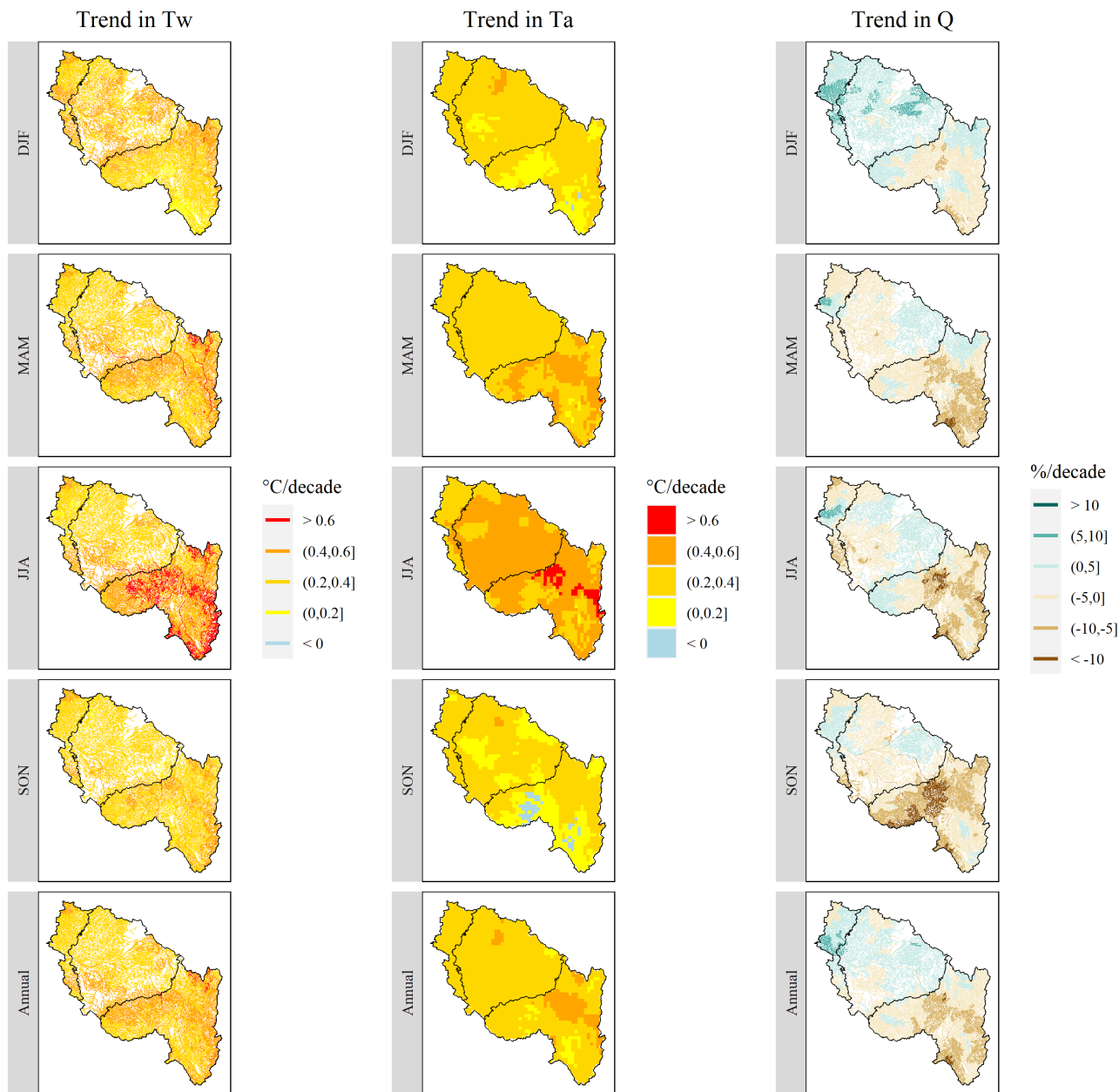
Figure 3. Spatial variability of trends in seasonal and annual Tw, Ta and Q over the 1963–2019 period, based on the Sen's Slope estimator. Solid black lines show the Hydro-Ecoregion (HER) delineation (see Fig. 1). The statistical significance of these trends is given in Fig. S5S12.

Tw (+0.08 ~~–~~ to +1.02 °C/decade) (Fig. 4). The greatest increase in ~~Tw~~ median Tw over the basin was found in summer (+0.44 °C/decade).

Overall, Tw trends were more spatially variable than Ta trends (see Figs. 3 and 4), suggesting the conditional influence of ~~Q trends (Fig. 4). Indeed, where~~ other factors like Q trends. Indeed, for the majority of reaches, Tw trends exceeded Ta trends ~~,~~ (see Fig. 5), with the exception of summer when it was the case for the half of the reaches. The difference between Tw and Ta trends could go up to 0.38 °C/decade (i.e. up to 2.2 °C over the whole 1963–2019 period) (see Fig. 5). At the majority of such reaches (where Tw trend > Ta trend) decreasing Q trends occurred coincidentally ~~at the majority of reaches~~ (43-94% of all reaches) for all seasons ~~–~~ (with the exception of winter~~– (43-72 %, depending on season;)~~ irrespective of whether all significant and non-significant trends were considered (Fig. 6, top) or only significant trends of all three variables (i.e. Tw, Ta and Q) were considered (Fig. 6, bottom). Of these specific reaches where ~~all factors converged (trend in Tw higher than trend in Ta , and decreasing trend in Q)~~ Tw trend > Ta trend and Q trend < 0, most were located in HER A ~~, especially in spring (52~~ (see Figs. S15 and S16). Moreover, wherever Tw trends ~~% of such reaches) and summer (79~~ < ~~% of such reaches)~~ Ta trend, increasing Q trends occurred coincidentally (see dark blue bars in Fig. 6), suggesting again the influence of Q trends as a possible explanation for discrepancy found between Tw and Ta trends.
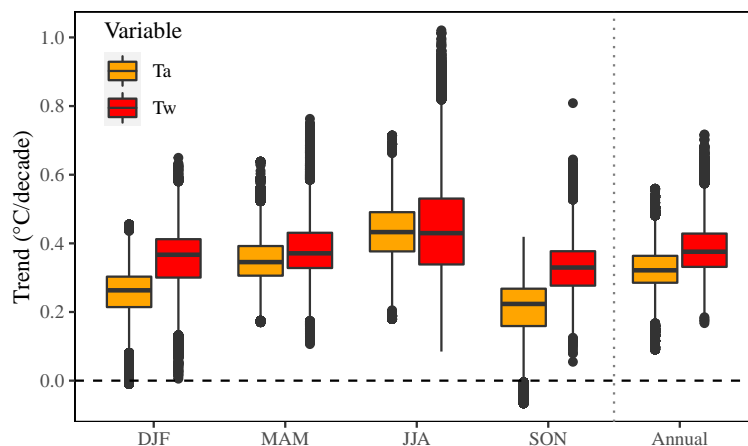
Figure 4. Distributions of seasonal and annual trends in Tw and Ta for all 52 278 reaches over the 1963–2019 period. Sen's slope is used as trend value estimate (see text). This representation includes both significant and non-significant trends.

~~Synchrony of annual anomalies~~ Temporal synchronicity

We observed strong positive correlations between seasonal and annual averages of Tw and Ta across seasons (r=+0.72 to +0.82 depending on the season; see Table 2). We further observed strong negative correlation between summer Tw and Q time series ~~. The strong positive correlation observed between winter Ta and Q results from the particular hydroclimate of winters in the Loire basin, where they are either either warm and wet or cold and dry.~~ (r=-0.40).
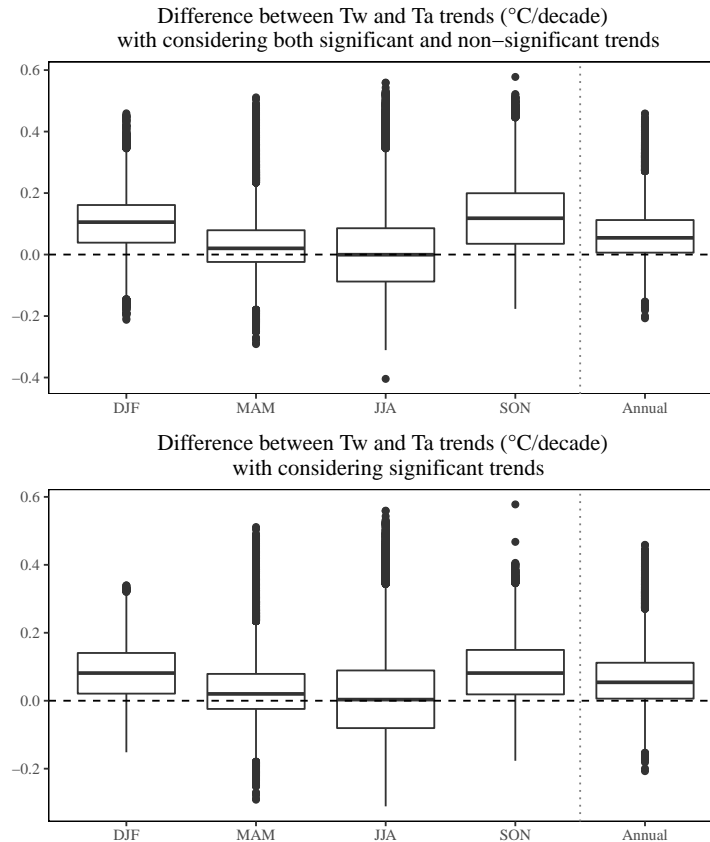
Figure 5. ~~Percentage of reaches with consistent 1963–2019 trends in~~ Difference between Tw ~~, Ta, and Q, categorised with respect to two criteria: (1) Tw trend >~~ Ta trend ~~, and (2) sign of Q trend~~at each reach in °C/decade for the whole 52 278 reaches.~~Sen's slope is used as trend value estimate.~~

~~Seasonal and annual times series of anomalies in Tw (), Ta () and relative Q (%) with respect to 1963–2019 averages. Grey intervals show the 5th and 95th percentiles across reaches, and the solid grey line depicts the median value. Note that Ta and Tw have the same scale.~~

Annual anomalies of Tw, Ta, and Q exhibited variable patterns, with Tw and Ta generally increasing and Q remaining
375 relatively stationary (Fig. ~~??~~S17). Tw anomalies were generally more variable than Ta, especially in summer, but both time series appeared to exhibit synchronous behavior. Change-point analysis supported this visual observation, where change-points in seasonal and annual averages were largely coincident across these time series (Fig. 7). Tw and Ta anomalies exhibited clear negative-to-positive change-points in the late 1980s at nearly all reaches, with median values ~~shifting~~ increasing by approximately +2 °C after the change-point. These change points were observed in all seasons, but were most pronounced
380 and synchronous around 1988 in spring and summer. The change-points detected in winter Tw and Ta time series were less concomitant, occurring mostly in the early 1990s (1992 and 1993) for Tw and in the late 1980s (1986-1989) for Ta. The fall
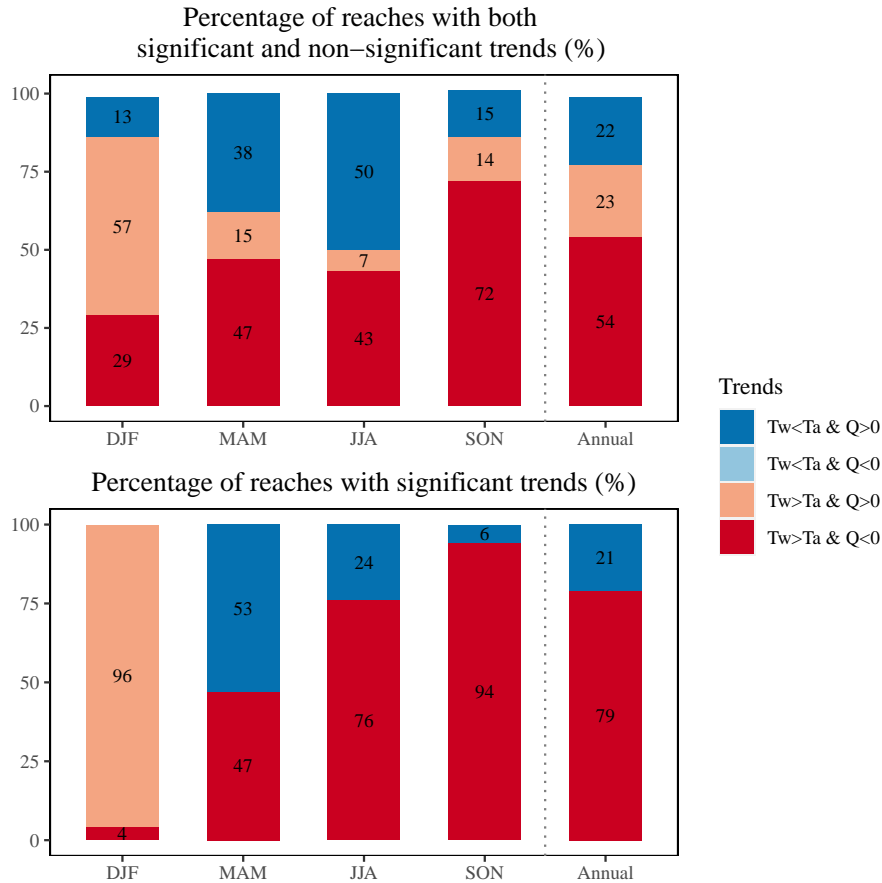
Figure 6. Percentage of reaches with consistent 1963–2019 trends in Tw, Ta, and Q, categorised with respect to two criteria: (1) comparison between Tw and Ta trends, and (2) sign of Q trend. Sen's slope is used as trend value estimate.

change-points were distributed between 1980 and 1994 for both Tw and Ta. The significant change-points in seasonal Q time series were detected for a substantially smaller proportion of reaches, e.g. less than 40 % of reaches for spring and summer. The majority of these reaches were located in HER A across seasons (66-86 % of such reaches), with the exception of winter (49 %)

385 (see Fig. ~~S8~~S18). In spring and summer, they occurred in the late 1980s, similarly to Tw and Ta. Conversely, the significant change-points detected in other seasons were much more scattered in time, probably due to the high interannual variability of Q.

Critically, the largest summer Tw and Ta positive anomalies over the study period were observed in 1976, 1994, 1995, 2003, 2005, 2006, 2015, 2017, 2018 and 2019, which corresponded to years with the largest negative anomalies in summer Q with

390 the exception of 1994 and 2018 (Fig. 8). Note that this signal was much less clear for the other seasons (see Fig. ~~S9~~S19).
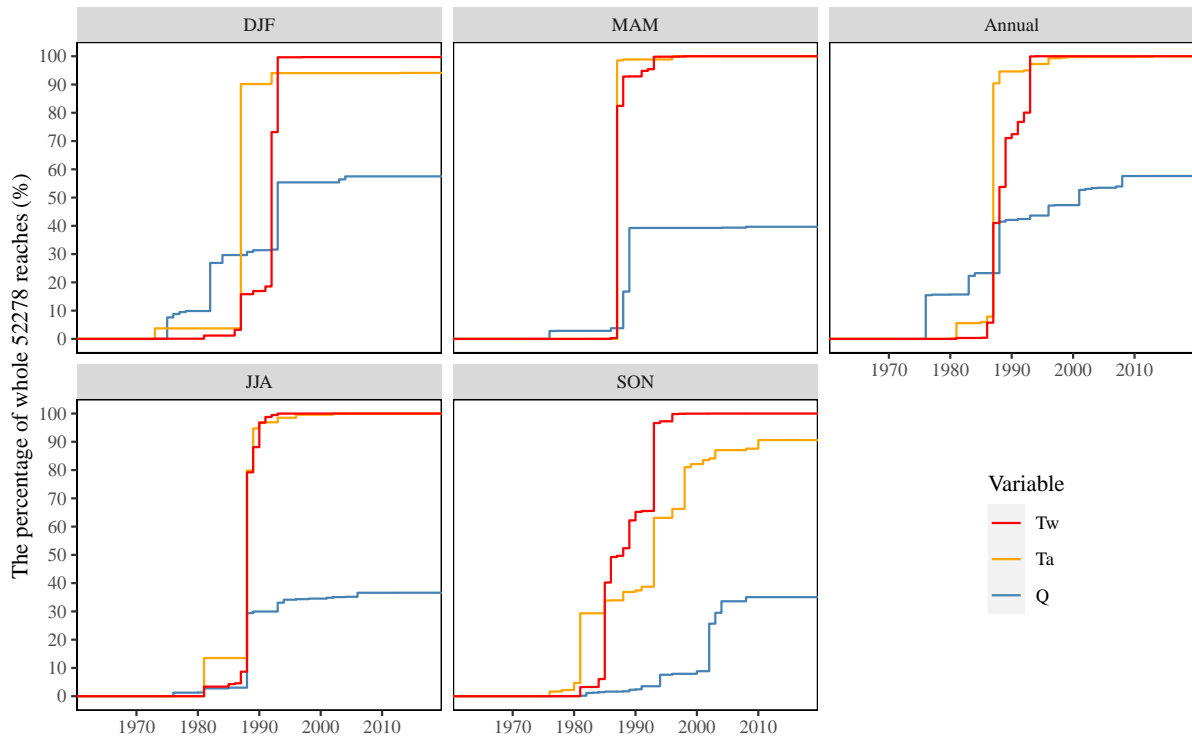
Figure 7. Change-point in Tw, Ta, and Q time series at the seasonal and annual scales, plotted as a proportion of reaches experiencing a shift in a given year. Only the first change-point detected at the 95% confidence level is considered, and non-significant change-points were removed, leading to curves not reaching 100 %.

4.4 Landscape drivers of Tw trends

4.4.1 Stream size and HER

Strahler order was strongly (p<0.001) and positively correlated with Tw trends ~~in spring and summer, but this effect was modulated by HER ,with HER A exhibiting the strongest correlations~~ (for all HERs in spring, and for HER A in summer
395 and fall and at annual scale. HER A exhibited the highest positive correlations in spring (r= +0.32) and summer (r=+0.15) (Fig. ~~??).~~ S20). In other words, larger rivers tended to exhibit the largest increases in spring and summer Tw, especially for reaches located in the HER A. There, median trends in spring (resp. summer) ranged from +0.37 to +0.55 °C/decade (resp. from +0.49 ~~)~~to +0.64 °C/decade~~for)~~ from small streams (Strahler order 1) to ~~+0.55 (resp. +0.64) for large streams~~ large rivers (Strahler order ≥ 5).

400   ~~Relationships between reach size and median trends in Tw across reaches over 1963–2019, by HER and by season. Correlations and associated p-values are shown in the top-left corner of each graph, and significant relationships at the 95 % confidence level are identified by full solid lines.~~
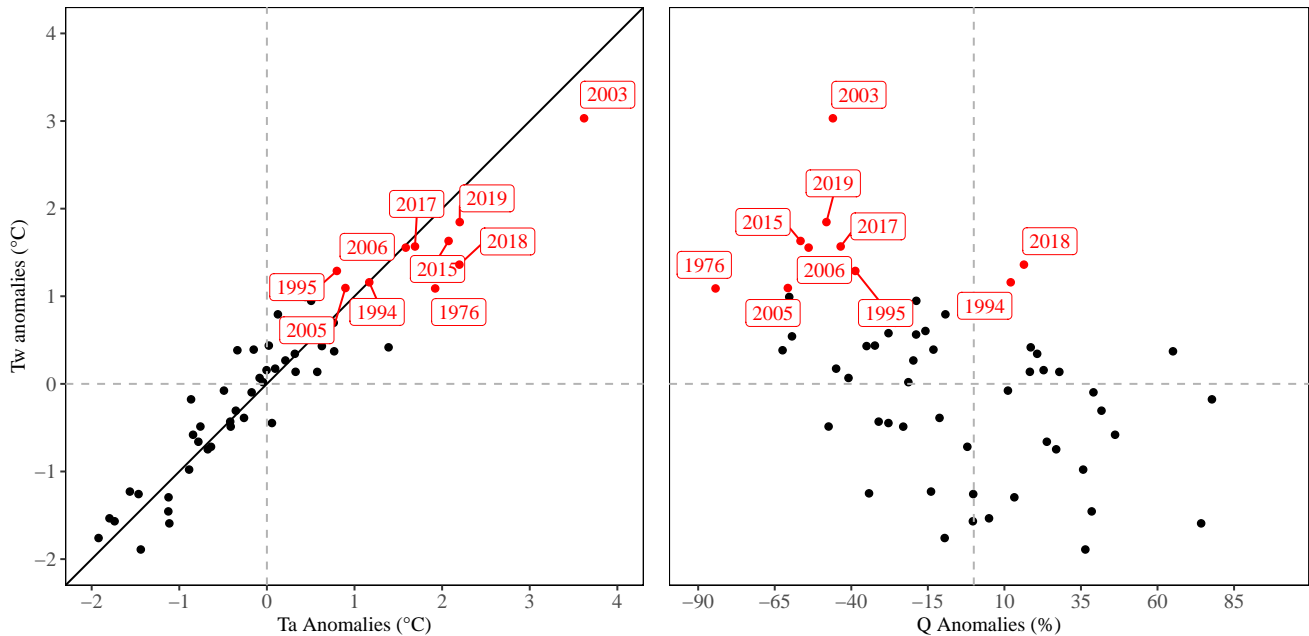
Figure 8. Relationship between summer anomalies in Tw on one side and summer Ta and Q anomalies on the other side. Individual years are identified from their median values across all reaches. Years with the highest anomalies in Tw (> +1 °C), and corresponding anomalies in Ta, and Q are identified in red.

4.4.2 Riparian shading and HER

4.4.3 ~~Riparian shading~~

405 For small streams, i.e. reaches located closer than 30 km from the source, the shading factor (SF~~and median~~) and trends in Tw were significantly (p<0.001) and negatively correlated ~~for all three HERs in spring~~in HER A in all seasons, as well as ~~for HER A in summer and at annual scale~~ in HER B and C in spring and in HER B in fall (Fig. 9). ~~The highest~~ Indeed, across seasons, the highest negative correlation was found in ~~summer in~~ HER A (r=-0.56 to -0.37 depending on the season). Unsurprisingly, the ~~influence of riparian vegetation shading on trends in Tw was more important in spring and summer. The~~ mitigating effect

410 of shading on trends in Tw for small streams was observed for all HERs in spring, and only for HER A in summer and, to a lesser extent, in fall and winter. The median spring Tw trend ~~in the HER A, B and C decreased by 12~~was mitigated by 0.12 ~~%, 5 % and 4 %, respectively,~~°C/decade from sparsely shaded reaches ($SF < 15\%$) to highly shaded reaches ($SF > 40\%$). For summer Tw in HER A, the median trends ~~were 16~~was mitigated by 0.16 ~~% lower between the lowest and~~ °C/decade from the lowest shaded reaches to the highest shaded reaches.
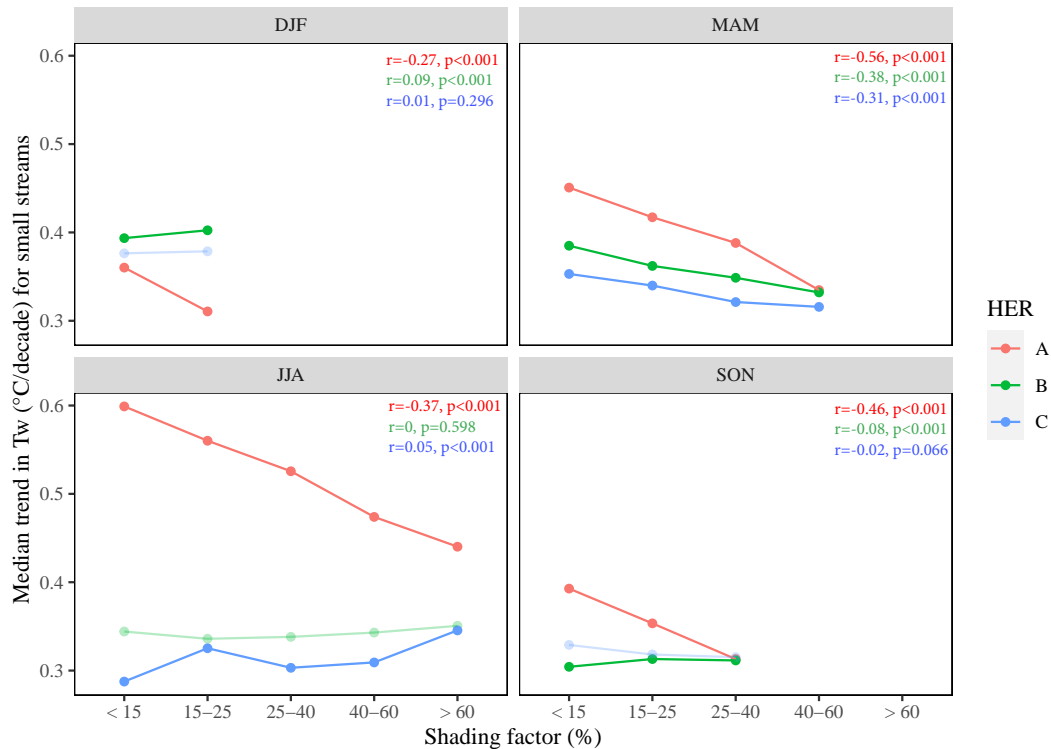
Figure 9. Relationships between shading factor and median trends in Tw over the 1963–2019 period for small streams, by HER and by season. Note that some shading factor classes are not observed in fall and winter. Correlations and associated p-values are shown on the ~~top-right~~ top-left corner of each graph, and significant relationships at the 95 % confidence level are identified by full solid lines.

5 Discussion

5.1 Quality and suitability of simulated Tw and Q

Although some biases were observed for both Q (Fig. S6) and Tw (Fig. ~~S2~~S9), we found ~~high~~ significant correlations between modeled and observed trends in seasonal and annual Q, with the exception of summer (Fig. ~~S3~~S10), and Tw, with the exception of fall (Fig. ~~S4), demonstrating the adequacy of the modelling approach for temporal trend analyses. For Q , although largely non-significant~~ S11). The low correlation value found in summer Q (Fig. ~~S5) , decreasing trends were observed for the majority of the reaches across seasons (66-83% of reaches, with the exception of winter, Fig. S7) strongly suggested an effect on Tw.~~ S10) originated from poor simulation at very few stations all located in HER B. Two of these stations gauged catchments where numerous small ponds were found and the highly decreasing observed trends might be due to the increasing evaporation from these ponds which were obviously not included in the EROS hydrological model. This was also true in a lesser extent for the other hydrometric station, in which a canal followed a large part of the course of the river and might play a similar role with respect to summer evaporation trends. Apart from these specific stations, in summer, a coherence as good as in other

seasons was found between trends in simulated and observed Q. Moreover, the spatial pattern in simulated Q trends, with significant decreases in the southern headwaters, was consistent with observations at the high-quality reference hydrometric stations ~~(Giuntoli et al., 2013).~~ (Giuntoli et al., 2013, their figure 5).

430 ## 5.2 ~~Agreement between trends in observed and simulated Tw~~

The low correlation between simulated and observed Tw trend found in fall (Fig. S11) originated from two stations with 8-13 years Tw data while such correlation was really good at stations on the Loire and Vienne rivers with longer (20-40 years) Tw data. Therefore, poor correlation in fall could be due to insufficient Tw data at these two stations. Moreover, consistent with Moatar and Gailhard (2006) and Arevalo et al. (2020), we found no trend (p>0.05) in both observation and simulation at Loire
435 (Dampierre) in winter.

5.2 Comparison with Tw trends in other European basins

T-NET simulations over the ~~1963–2019~~ 1963–2019 period showed significantly increasing trends in Tw for almost all reaches over the Loire basin across seasons ~~,~~ (see Fig. 3, left, and Fig. S12, left), with an increase of +0.38°C/decade ~~increase~~ on average at the annual scale. To the best of authors' knowledge, the present study was one of the ~~very~~ few studies used modeled
440 Tw to investigate past ~~trend~~ trends at a large scale (but see Van Vliet et al., 2011; Isaak et al., 2012, 2017). Table 3, summarizing recently published findings based on observations, demonstrate that the present results are consistent with trends observed in other European ~~basin~~ basins with clear increases in Tw over the recent decades. It also shows that the much larger scale and finer spatial resolution of the current study clearly stands out as unique. Although start year, end year and length of the study period can have ~~can have~~ a significant influence on trend estimates and trend detection (Arora et al., 2016), comparing trends
445 with other studies conducted over different periods ~~give~~ gives us a comprehensive view upon the overall magnitude of changes in Tw and possible related drivers.

Global-scale stream temperature modelling suggests trends in annual averages ranging from +0.2 to +0.5°C/decade over France (Wanders et al., 2019), which is consistent with our findings (mostly in the range of +0.2 ~~–~~ to +0.4°C/decade, Fig. ~~S6~~S13). We found more pronounced trends in spring and summer, which was also found in other parts of Europe (e.g. Kę-
450 dra, 2020; Arora et al., 2016; Michel et al., 2020). Considerable discrepancies were also found between Tw and Ta trends across seasons for the majority of the reaches (see ~~Fig~~Figs. 3, and ~~6~~5), which is a common finding for other sites around the world ~~(Arora et al., 2016; Wanders et al., 2019)~~(Arora et al., 2016; Wanders et al., 2019). This highlights that changes in Ta may not be the only driver of changes in natural Tw.

5.3 Drivers and spatial patterns of trends in Tw

455 ~~The~~ Consistent with our findings (see Fig. 5), Moatar and Gailhard (2006) found Tw increased faster than Ta in spring and summer and at the annual scale for all 4 stations on the Loire River. Arora et al. (2016) also found Tw trends > Ta trends in summer. In Switzerland, Michel et al. (2020) described an increase of +0.33 ± 0.03°C/decade in Tw, resulting from the joint

effects of an increase in Ta (+0.39 ± 0.14°C/decade) and a decrease in Q (−10.1 ± 4.6%/decade) over the 1979–2018 period. In contrast with our results, they found Tw trends lower than Ta trends due to influence of snow melt and glacier melt in Alpine

460 catchments. Consistent with their findings, Orr et al. (2015) also found Tw trends < Ta trends in UK. They suggested the such difference between Tw and Tw trends could be as a result of different processes driving Tw. In the current study, we found spatial coherence between trends in Tw and trends in Ta and Q. Indeed, the greatest increases in Tw (up to +1 °C/decade) were predominately located in the southern ~~headwaters~~ part of the basin, in HER A (Massif Central) where a greater increase in Ta (up to +0.71 °C/decade) and a greater decrease in Q (up to -16 %/decade) occurred jointly. We also found, at the majority of

465 reaches where Tw trend>Ta trend, decreasing Q trends occurred coincidentally for all seasons (with the exception of winter) (Fig. 6).

The decrease in Q could itself be due to a significant increase in potential evapotranspiration (PET) (up to +10 %) over the whole of basin and a decrease in total precipitation (P) (up to -5 %/decade) (Figs. ~~S10 and S11~~S21 and S22). Such trends, computed here based on variables from the Safran surface meteorological reanalysis (Vidal et al., 2010), are consistent with

470 larger-scale studies (see e.g. Spinoni et al., 2017; Tramblay et al., 2020; Hobeichi et al., 2021). Moreover, Vicente-Serrano et al. (2019) attributed annual streamflow trends in southern France mostly to trends in precipitation and potential evapotranspiration, as opposed to irrigation and land-use changes that have additional strong effects e.g. in the Iberian peninsula. ~~In Switzerland, Michel et al. (2020) described an increase of +0.33 ± 0.03in Tw , resulting from the joint effects of increasing in Ta (+0.39 ± 0.14) and decreasing in Q (−10.1 ± 4.6) over the 1979–2018 period. In contrast with our results, they found Tw~~

475 ~~trends lower than Ta trends due to influence of snow melt and glacier melt. Trends in Tw might also be explained by trends in additional drivers, like shortwave radiation (Wanders et al., 2019), which is the dominant flux at air-water surface, and is notably increasing over Europe (Sanchez-Lorenzo et al., 2015). This might explain discrepancies~~ We also observed, for the majority of reaches where Tw increased less than Ta, an increase in Q occurred jointly suggesting that increase in Q or in other words increase in thermal inertia could also explain the discrepancy between Tw and Ta trends ~~in spring and summer, when no~~

480 ~~decreasing trend in Q are found~~ at these reaches (see Fig. ~~3~~6).

~~Strong~~ A strong synchronicity between Ta and Tw anomalies was observed in the present study in the warmest years, and these years were also among those with the largest negative Q anomalies (see Fig. 8). Indeed, increase in summer Tw could be due to co-occurrence with the increase in summer Ta (average correlation: +0.82), and with the decrease in summer Q (average correlation: -0.40). These findings are consistent with those of Michel et al. (2020): average Tw-Ta correlation: +0.61, and

485 average Tw-Q correlation: -0.66. For the middle Loire ~~river~~River, Moatar and Gailhard (2006) found that the increase in Ta (resp. decrease in Q) explain 60 % (resp. 40 %) of the increase in Tw. Moreover, the significant change-point in Tw, Ta and Q time series in the late 1980s has also been found in other studies in Europe (Moatar and Gailhard, 2006; Arora et al., 2016; Zobrist et al., 2018; Ptak et al., 2019b; Michel et al., 2020). Long-term observational Tw time series like that of the Loire at Dampierre also display a similar change-point.

490 Trends in Tw might also be explained by trends in additional drivers (not considered directly in the current study), like shortwave radiation (Wanders et al., 2019), which is the dominant flux at air-water surface, and is notably increasing over

Europe (Sanchez-Lorenzo et al., 2015). This might explain why Tw increased faster than Ta in spring, summer and fall, when no decreasing trend in Q were found (see Fig. 6).

The current study suggests that Ta and Q could exert a joint influence on Tw, based on an analysis of the spatial coherence and temporal synchronicity of these variables. Assessing causal influence of these factors on Tw trends goes beyond the scope of this paper and is left for future research. In this regard, one could devise a formal attribution framework where one may e.g. remove trends in Q and trends in Ta alternatively in T-NET inputs.

5.4 Natural trends and anthropogenic influence on Tw

Natural Tw time series were used in the current study for detecting trends, as both EROS and T-NET models are used in a non-influenced set-up (see Sect. 3.1). However, anthropogenic impoundments (e.g. large dams, small reservoirs, and ponds) influence downstream Tw regimes in a diversity of ways that depend on their structure and position along the river continuum (Seyedhashemi et al., 2020). In this regard, on the one hand, large dams, by releasing cold hypolimnetic water in summer, can lower downstream Tw (Olden and Naiman, 2010), and mitigate increasing trend in Tw (Cheng et al., 2020). Nevertheless, it is anticipated that a considerable proportion of streams regulated by large dams may still experience high temperatures and low flows under future climate change (Cheng et al., 2020). The mitigating influence of dams could be of importance for streams in the southern headwaters of the Loire basin since this area both experienced the greatest Tw trends and gathers most of existing large dams.

On the other hand, ponds and shallow reservoirs, by releasing warm water can increase downstream Tw (Chandesris et al., 2019; Seyedhashemi et al., 2020; Zaidel et al., 2020) and exacerbate increasing trends in Tw (Wanders et al., 2019; Michel et al., 2020). Nevertheless, the warming effect can be local, and unregulated streams being located closer to such regulated streams may show limited to no warming (Wanders et al., 2019). The warming effect of such surface waters in the current study seem more can be significant for streams located in lowlands in the middle and north of the Loire River basin where most of the shallow reservoirs and ponds are located. In these streams, anthropogenically-induced trends in Tw may be greater than natural ones, and the warming process can get worse through the increasing demand for storing water in small reservoirs for irrigation. Nevertheless, the warming effect can also be local, and streams being located closer to such regulated streams may show limited to no warming (Wanders et al., 2019).

Note that although there are nuclear power plants in the Loire basin, their impacts on Tw is considered negligible according to Moatar and Gailhard (2006) and Bustillo et al. (2014). Moreover, it was observed in the current study that the Tw trend at Belleville located in upstream of power plants and consequently, not influenced by them, had the same trend magnitude as the other three stations located downstream (see Fig. 2), showing a negligible influence of nuclear power plants on Tw trends.

5.5 Implications for river management and aquatic biota

The removal of riparian vegetation can increase Tw (Caissie, 2006), and changes in Tw can be even more sensitive to changes in riparian vegetation than to changes in Ta or Q (Wondzell et al., 2019). We showed that in small streams, an increase of > 25 % of riparian shading could decrease (from 15% to 40%) could mitigate the median trend in spring and summer Tw by

525 ~~5–16~~up to 16 ~~%~~°C/decade (Fig. 9). Spring and summer Tw trends were more pronounced in large rivers, especially in the south of the basin, with a difference in median Tw trends of up to +0.18 °C/decade (Fig. ~~??~~S20), probably due to decrease in Q (up to -2 ~~%/decade, see Fig. S12),~~S23), a greater thermal sensitivity, and the absence of mitigating factors like riparian vegetation shading or groundwater inputs (Kelleher et al., 2012; Beaufort et al., 2020).

Restoring riparian vegetation and shading can therefore substantially mitigate future increases in Tw. In addition, riparian

530 restoration may lessen the impacts of climate change on flood damage to human infrastructure, on riparian biodiversity, on ecosystem vulnerability and on changes in Q (Palmer et al., 2009; Seavy et al., 2009; Perry et al., 2015). However, riparian restoration is not an easy task since the survival, persistence, growth rate of planted ~~species~~ trees as well as required time for thermal regime recovery under possibly severe future conditions should be studied beforehand (Perry et al., 2015). For instance, it may take between 5 and 15 years for rivers to recover their thermal regime following vegetation growth (Edmonds

535 et al., 2000; Caissie, 2006). Moreover, the efficacy of riparian planting is also highly dependent upon the type and structure of forest stands (Dugdale et al., 2018), and this should also be considered in long-term projects.

Stream warming affects cold-water fish populations negatively at the warmer boundaries of their habitat (Hari et al., 2006). Furthermore, changes in spawning and migration timing (McCann et al., 2018; Arevalo et al., 2020), decreases in habitat availability and freshwater quality for organisms (Lennox et al., 2019), and shifts in species distribution (Comte et al., 2013)

540 are already observed as consequences of the long-term increase in Tw. Some major changes in fish density and community structure has already been reported in large rivers over France (Maire et al., 2019) for which we also found greater trends in Tw compared to small ones. Therefore, physical process-based thermal models like T-NET can also be used to assess the various stresses on freshwater habitat sustainability due to changes in Q and Tw (Morales-Marín et al., 2019).

6 Conclusions

545 Regional trends in Tw at the reach resolution were detected and assessed by using the T-NET physical process-based model coupled with the EROS hydrological model over the Loire basin. Using model outputs across 52 278 reaches over the Loire basin, for 3 variables (Ta, Q, and Tw), and 5 time scales (seasons plus annual), we found consistent increasing Tw trends at the scale of the entire Loire River basin, regardless of the season. Critically, the rate of warming for stream temperature was in the majority of ~~cases~~ reaches higher than the rate of atmospheric warming, suggesting a decoupling of thermal trajectories linked

550 to decreasing Q, especially in the southern ~~headwaters~~part of the basin supported by observed coherent spatial and temporal patterns, and well-understood physical processes. Moreover, in the southern part of the basin, Tw trends in all seasons except winter were greater in rivers with Strahler order ≥ 5, which we attributed to the mitigation effect of riparian shading for ~~large~~ small rivers.

The synchronicity of extreme events of low flows and high ~~air~~ stream temperature in the southern ~~headwaters~~ part of the

555 basin will likely generate a double penalty for existing cold-water aquatic communities. However, riparian shading in small ~~mountainous streams~~ streams in the southern part of the basin may mitigate such warming. These findings underscore that ~~Ta~~ air temperature alone is likely not an adequate proxy to explain stresses and shifts experienced by aquatic communities over

time and space, especially in regions with more pronounced stream warming, and thus there is a need to grow and maintain Tw sensor networks. It also highlights that the physical process-based thermal models like T-NET can also be used to assess the various stresses on freshwater habitat sustainability due to changes in Q and Tw. This knowledge can help develop appropriate management strategies to conserve thermal refugia and mitigate extreme thermal events induced by climate change.

Data availability. The seasonal and annual Tw and Q time series at 67 stations (see Tables 1 and S5) can be downloaded from: https://doi.org/10.15454/PTY9R7. Data for other reaches in the basin and codes are available from the corresponding author, [HS], upon reasonable request.

Author contributions. HS: Conceptualization, Methodology, Software, Formal analysis, Writing - original draft preparation JPV: Conceptualization, Methodology, Writing - review and editing; JD: Methodology; Writing - review and editing; DT: Resources, Writing - review; CM: Resources; FH: Resources; AM: Writing - review and editing; FM: Conceptualization, Methodology, Writing - review and editing, Supervision

Competing interests. The authors declare that they have no conflict of interest.

Acknowledgements. This work was realized in the course of a doctoral project at University of Tours, funded by European Regional Development Fund (Fonds Européen de développement Régional-FEDER) POI FEDER Loire n°2017- EX001784, Le plan Loire grandeur nature, Agence de l'eau Loire-Bretagne (AELB) and EDF (Hynes Team). The SAFRAN database was provided by the French national meteorological service (Météo-France). ~~Stream temperature data were provided by the Office français de la biodiversité (OFB), Fédération de Pêche (fishing federation).~~ We are grateful to Electricité de France (French Electricity, EDF) for providing long-term data on observed stream temperature and naturalized streamflows. We also thank André Chandesris for his assistance in the incorporation of vegetation cover into the T-NET thermal model.

References

Allen, R. G., Pereira, L. S., Raes, D., and Smith, M.: Crop Evapotranspiration – Guidelines for computing crop water requirements, FAO Irrigation and Drainage Paper 56, FAO, http://www.kimberly.uidaho.edu/water/fao56/, 1998.

580 Arevalo, E., Lassalle, G., Tétard, S., Maire, A., Sauquet, E., Lambert, P., Paumier, A., Villeneuve, B., and Drouineau, H.: An innovative bivariate approach to detect joint temporal trends in environmental conditions: Application to large French rivers and diadromous fish, Science of the Total Environment, 748, 141 260, https://doi.org/10.1016/j.scitotenv.2020.141260, 2020.

Arismendi, I., Johnson, S. L., Dunham, J. B., Haggerty, R., and Hockman-Wert, D.: The paradox of cooling streams in a warming world: regional climate trends do not parallel variable local trends in stream temperature in the Pacific continental United States, Geophysical

585 Research Letters, 39, https://doi.org/10.1029/2012GL051448, 2012.

Arismendi, I., Johnson, S. L., Dunham, J. B., and Haggerty, R.: Descriptors of natural thermal regimes in streams and their responsiveness to change in the Pacific Northwest of North America, Freshwater Biology, 58, 880–894, https://doi.org/10.1111/fwb.12094, 2013a.

Arismendi, I., Safeeq, M., Johnson, S. L., Dunham, J. B., and Haggerty, R.: Increasing synchrony of high temperature and low flow in western North American streams: double trouble for coldwater biota?, Hydrobiologia, 712, 61–70, https://doi.org/10.1007/s10750-012-

590 1327-2, 2013b.

Arismendi, I., Safeeq, M., Dunham, J. B., and Johnson, S. L.: Can air temperature be used to project influences of climate change on stream temperature?, Environmental Research Letters, 9, 084 015, https://doi.org/10.1088/1748-9326/9/8/084015, 2014.

Arora, R., Tockner, K., and Venohr, M.: Changing river temperatures in northern Germany: trends and drivers of change, Hydrological Processes, 30, 3084–3096, https://doi.org/10.1002/hyp.10849, 2016.

595 Bauer, D. F.: Constructing confidence sets using rank statistics, Journal of the American Statistical Association, 67, 687–690, https://doi.org/10.1080/01621459.1972.10481279, 1972.

Beaufort, A., Curie, F., Moatar, F., Ducharne, A., Melin, E., and Thiéry, D.: T-NET, a dynamic model for simulating daily stream temperature at the regional scale based on a network topology, Hydrological Processes, 30, 2196–2210, https://doi.org/10.1002/hyp.10787, 2016.

Beaufort, A., Moatar, F., Sauquet, E., Loicq, P., and Hannah, D. M.: Influence of landscape and hydrological factors on stream–air temperature

600 relationships at regional scale, Hydrological Processes, 34, 583–597, https://doi.org/10.1002/hyp.13608, 2020.

Benyahya, L., Caissie, D., St-Hilaire, A., Ouarda, T. B., and Bobée, B.: A review of statistical water temperature models, Canadian Water Resources Journal, 32, 179–192, https://doi.org/10.4296/cwrj3203179, 2007.

Blöschl, G., Hall, J., Viglione, A., Perdigão, R. A., Parajka, J., Merz, B., Lun, D., Arheimer, B., Aronica, G. T., Bilibashi, A., et al.: Changing climate both increases and decreases European river floods, Nature, 573, 108–111, https://doi.org/10.1038/s41586-019-1495-6, 2019.

605 Bruno, D., Belmar, O., Maire, A., Morel, A., Dumont, B., and Datry, T.: Structural and functional responses of invertebrate communities to climate change and flow regulation in alpine catchments, Global change biology, 25, 1612–1628, https://doi.org/10.1111/gcb.14581, 2019.

Buisson, L. and Grenouillet, G.: Contrasted impacts of climate change on stream fish assemblages along an environmental gradient, Diversity and Distributions, 15, 613–626, https://doi.org/10.1111/j.1472-4642.2009.00565.x, 2009.

610 Buisson, L., Blanc, L., and Grenouillet, G.: Modelling stream fish species distribution in a river network: the relative effects of temperature versus physical factors, Ecology of Freshwater Fish, 17, 244–257, https://doi.org/10.1111/j.1600-0633.2007.00276.x, 2008.

Bustillo, V., Moatar, F., Ducharne, A., Thiéry, D., and Poirel, A.: A multimodel comparison for assessing water temperatures under changing climate conditions via the equilibrium temperature concept: case study of the Middle Loire River, France, Hydrological Processes, 28, 1507–1524, https://doi.org/https://doi.org/10.1002/hyp.9683, 2014.

615 Caissie, D.: The thermal regime of rivers: a review, Freshwater biology, 51, 1389–1406, https://doi.org/10.1111/j.1365-2427.2006.01597.x, 2006.

Caissie, D., Satish, M. G., and El-Jabi, N.: Predicting water temperatures using a deterministic model: Application on Miramichi River catchments (New Brunswick, Canada), Journal of Hydrology, 336, 303–315, https://doi.org/10.1016/j.jhydrol.2007.01.008, 2007.

Chandesris, A., Van Looy, K., Diamond, J. S., and Souchon, Y.: Small dams alter thermal regimes of downstream water., Hydrology & Earth
620 System Sciences, 23, https://doi.org/10.5194/hess-23-4509-2019, 2019.

Cheng, Y., Voisin, N., Yearsley, J. R., and Nijssen, B.: Reservoirs modify river thermal regime sensitivity to climate change: a case study in the southeastern United States, Water Resources Research, 56, e2019WR025 784, https://doi.org/10.1029/2019WR025784, 2020.

Comte, L., Buisson, L., Daufresne, M., and Grenouillet, G.: Climate-induced changes in the distribution of freshwater fish: observed and predicted trends, Freshwater Biology, 58, 625–639, https://doi.org/10.1111/fwb.12081, 2013.

625 Dan Moore, R., Spittlehouse, D., and Story, A.: Riparian microclimate and stream temperature response to forest harvesting: A review, JAWRA Journal of the American Water Resources Association, 41, 813–834, https://doi.org/10.1111/j.1752-1688.2005.tb03772.x, 2005.

Domisch, S., Araújo, M. B., Bonada, N., Pauls, S. U., Jähnig, S. C., and Haase, P.: Modelling distribution in E uropean stream macroinvertebrates under future climates, Global Change Biology, 19, 752–762, https://doi.org/10.1111/gcb.12107, 2013.

Ducharne, A.: Importance of stream temperature to climate change impact on water quality, Hydrology and Earth System Sciences, 12,
630 797–810, https://doi.org/https://doi.org/10.5194/hess-12-797-2008, 2008.

Ducharne, A., Sauquet, E., Habets, F., Déqué, M., Gascoin, S., Hachour, A., Martin, E., Oudin, L., Pagé, C., Terray, L., et al.: Evolution potentielle du régime des crues de la Seine sous changement climatique, La Houille Blanche, pp. 51–57, https://doi.org/https://doi.org/10.1051/lhb/2011006, 2011.

Dugdale, S. J., Hannah, D. M., and Malcolm, I. A.: River temperature modelling: A review of process-based approaches and future directions,
635 Earth-Science Reviews, 175, 97–113, https://doi.org/10.1016/j.earscirev.2017.10.009, 2017.

Dugdale, S. J., Malcolm, I. A., Kantola, K., and Hannah, D. M.: Stream temperature under contrasting riparian forest cover: Understanding thermal dynamics and heat exchange processes, Science of The Total Environment, 610, 1375–1389, https://doi.org/10.1016/j.scitotenv.2017.08.198, 2018.

Edmonds, R., Murray, G., and Marra, J.: Influence of partial harvesting on stream temperatures, chemistry, and turbidity in forests on the
640 western Olympic Peninsula, Washington, WSU Press, http://hdl.handle.net/2376/1065, 2000.

Floury, M., Usseglio-Polatera, P., Ferreol, M., Delattre, C., and Souchon, Y.: Global climate change in large E uropean rivers: long-term effects on macroinvertebrate communities and potential local confounding factors, Global change biology, 19, 1085–1099, https://doi.org/10.1111/gcb.12124, 2013.

Giuntoli, I., Renard, B., Vidal, J.-P., and Bard, A.: Low flows in France and their relationship to large-scale climate indices, Journal of
645 Hydrology, 482, 105–118, https://doi.org/10.1016/j.jhydrol.2012.12.038, 2013.

Habets, F., Boé, J., Déqué, M., Ducharne, A., Gascoin, S., Hachour, A., Martin, E., Pagé, C., Sauquet, E., Terray, L., et al.: Impact of climate change on the hydrogeology of two basins in northern France, Climatic change, 121, 771–785, https://doi.org/10.1007/s10584-013-0934-x, 2013.

Hannah, D. M. and Garner, G.: River water temperature in the United Kingdom: changes over the 20th century and possible changes over the 21st century, Progress in Physical Geography, 39, 68–92, https://doi.org/10.1177/2F0309133314550669, 2015.

Hannah, D. M., Malcolm, I. A., Soulsby, C., and Youngson, A. F.: Heat exchanges and temperatures within a salmon spawning stream in the Cairngorms, Scotland: seasonal and sub-seasonal dynamics, River Research and Applications, 20, 635–652, https://doi.org/10.1002/rra.771, 2004.

Hari, R. E., Livingstone, D. M., Siber, R., BURKHARDT-HOLM, P., and Guettinger, H.: Consequences of climatic change for water temperature and brown trout populations in Alpine rivers and streams, Global Change Biology, 12, 10–26, https://doi.org/10.1111/j.1365-2486.2005.001051.x, 2006.

Hobeichi, S., Abramowitz, G., and Evans, J. P.: Robust historical evapotranspiration trends across climate regimes, Hydrology and Earth System Sciences, 25, 3855–3874, https://doi.org/10.5194/hess-25-3855-2021, 2021.

Huntington, T. G.: Evidence for intensification of the global water cycle: review and synthesis, Journal of Hydrology, 319, 83–95, https://doi.org/10.1016/j.jhydrol.2005.07.003, 2006.

Hutchison, B. A. and Matt, D. R.: The distribution of solar radiation within a deciduous forest, Ecological Monographs, 47, 185–207, https://doi.org/10.2307/1942616, 1977.

IGN: Descriptif technique BD TOPO, Tech. rep., Institut Gógraphique National, https://www.cc-saulnois.fr/sig/documents/BDTOPO/DC_BDTOPO_2.pdf, 2008.

IGN: Descriptif technique BD ALTI, Tech. rep., Institut Gógraphique National, https://geoservices.ign.fr/ressources_documentaires/Espace_documentaire/MODELES_3D/BDALTIV2/DC_BDALTI_2-0.pdf, 2011.

Isaak, D., Wollrab, S., Horan, D., and Chandler, G.: Climate change effects on stream and river temperatures across the northwest US from 1980–2009 and implications for salmonid fishes, Climatic change, 113, 499–524, https://doi.org/10.1007/s10584-011-0326-z, 2012.

Isaak, D. J., Wenger, S. J., Peterson, E. E., Ver Hoef, J. M., Nagel, D. E., Luce, C. H., Hostetler, S. W., Dunham, J. B., Roper, B. B., Wollrab, S. P., et al.: The NorWeST summer stream temperature model and scenarios for the western US: A crowd-sourced database and new geospatial tools foster a user community and predict broad climate warming of rivers and streams, Water Resources Research, 53, 9181–9205, https://doi.org/10.1002/2017WR020969, 2017.

Jackson, F., Hannah, D. M., Fryer, R., Millar, C., and Malcolm, I.: Development of spatial regression models for predicting summer river temperatures from landscape characteristics: Implications for land and fisheries management, Hydrological processes, 31, 1225–1238, https://doi.org/10.1002/hyp.11087, 2017.

Jackson, F. L., Fryer, R. J., Hannah, D. M., Millar, C. P., and Malcolm, I. A.: A spatio-temporal statistical model of maximum daily river temperatures to inform the management of Scotland's Atlantic salmon rivers under climate change, Science of the Total Environment, 612, 1543–1558, https://doi.org/10.1016/j.scitotenv.2017.09.010, 2018.

Johnson, S. L.: Factors influencing stream temperatures in small streams: substrate effects and a shading experiment, Canadian Journal of Fisheries and Aquatic Sciences, 61, 913–923, https://doi.org/10.1139/f04-040, 2004.

Kaushal, S. S., Likens, G. E., Jaworski, N. A., Pace, M. L., Sides, A. M., Seekell, D., Belt, K. T., Secor, D. H., and Wingate, R. L.: Rising stream and river temperatures in the United States, Frontiers in Ecology and the Environment, 8, 461–466, https://doi.org/10.1890/090037, 2010.

Kędra, M.: Regional response to global warming: Water temperature trends in semi-natural mountain river systems, Water, 12, 283, https://doi.org/10.3390/w12010283, 2020.

Kelleher, C., Wagener, T., Gooseff, M., McGlynn, B., McGuire, K., and Marshall, L.: Investigating controls on the thermal sensitivity of Pennsylvania streams, Hydrological Processes, 26, 771–785, https://doi.org/10.1002/hyp.8186, 2012.

Kirk, M. A. and Rahel, F. J.: Air temperatures over-predict changes to stream fish assemblages with climate warming compared with water temperatures, Ecological Applications, 32, e02 465, https://doi.org/https://doi.org/10.1002/eap.2465, 2022.

690   Kurylyk, B. L., Bourque, C.-A., and MacQuarrie, K. T.: Potential surface temperature and shallow groundwater temperature response to climate change: an example from a small forested catchment in east-central New Brunswick (Canada), Hydrology and Earth System Sciences, 17, 2701–2716, https://doi.org/10.5194/hess-17-2701-2013, 2013.

Kurylyk, B. L., MacQuarrie, K. T., and Voss, C. I.: Climate change impacts on the temperature and magnitude of groundwater discharge from shallow, unconfined aquifers, Water Resources Research, 50, 3253–3274, https://doi.org/10.1002/2013WR014588, 2014.

695   Lennox, R. J., Crook, D. A., Moyle, P. B., Struthers, D. P., and Cooke, S. J.: Toward a better understanding of freshwater fish responses to an increasingly drought-stricken world, Reviews in fish biology and fisheries, 29, 71–92, https://doi.org/10.1007/s11160-018-09545-9, 2019.

Li, G., Jackson, C. R., and Kraseski, K. A.: Modeled riparian stream shading: Agreement with field measurements and sensitivity to riparian conditions, Journal of hydrology, 428, 142–151, https://doi.org/10.1016/j.jhydrol.2012.01.032, 2012.

Loicq, P., Moatar, F., Jullian, Y., Dugdale, S. J., and Hannah, D. M.: Improving representation of riparian vegetation
700   shading in a regional stream temperature model using LiDAR data, Science of the total environment, 624, 480–490, https://doi.org/10.1016/j.scitotenv.2017.12.129, 2018.

Maire, A., Thierry, E., Viechtbauer, W., and Daufresne, M.: Poleward shift in large-river fish communities detected with a novel meta-analysis framework, Freshwater Biology, 64, 1143–1156, https://doi.org/10.1111/fwb.13291, 2019.

Majdi, N., Uthoff, J., Traunspurger, W., Laffaille, P., and Maire, A.: Effect of water warming on the structure of biofilm-dwelling communi-
705   ties, Ecological Indicators, 117, 106 622, https://doi.org/10.1016/j.ecolind.2020.106622, 2020.

Mann, H. B.: Nonparametric tests against trend, Econometrica: Journal of the econometric society, pp. 245–259, https://doi.org/10.2307/1907187, 1945.

Mantua, N., Tohver, I., and Hamlet, A.: Climate change impacts on streamflow extremes and summertime stream temperature and their possible consequences for freshwater salmon habitat in Washington State, Climatic Change, 102, 187–223, https://doi.org/10.1007/s10584-
710   010-9845-2, 2010.

Mayer, T. D.: Controls of summer stream temperature in the Pacific Northwest, Journal of Hydrology, 475, 323–335, https://doi.org/10.1016/j.jhydrol.2012.10.012, 2012.

McCann, E. L., Johnson, N. S., and Pangle, K. L.: Corresponding long-term shifts in stream temperature and invasive fish migration, Canadian Journal of Fisheries and Aquatic Sciences, 75, 772–778, https://doi.org/10.1139/cjfas-2017-0195, 2018.

715   Meisner, J. D.: Potential loss of thermal habitat for brook trout, due to climatic warming, in two southern Ontario streams, Transactions of the American Fisheries Society, 119, 282–291, https://doi.org/10.1577/1548-8659(1990)119%3C0282:PLOTHF%3E2.3.CO;2, 1990.

Michel, A., Brauchli, T., Lehning, M., Schaefli, B., and Huwald, H.: Stream temperature and discharge evolution in Switzerland over the last 50 years: annual and seasonal behaviour., Hydrology & Earth System Sciences, 24, https://doi.org/10.5194/hess-24-115-2020, 2020.

Moatar, F. and Dupont, N.: La Loire fluviale et estuarienne: un milieu en évolution, Editions Quae, https://www.quae.com/produit/1334/
720   9782759224036/la-loire-fluviale-et-estuarienne, 2016.

Moatar, F. and Gailhard, J.: Water temperature behaviour in the River Loire since 1976 and 1881, Comptes Rendus Geoscience, 338, 319–328, https://doi.org/10.1016/j.crte.2006.02.011, 2006.

Mohseni, O., Erickson, T. R., and Stefan, H. G.: Sensitivity of stream temperatures in the United States to air temperatures projected under a global warming scenario, Water Resources Research, 35, 3723–3733, https://doi.org/10.1029/1999WR900193, 1999.

725 Morales-Marín, L., Rokaya, P., Sanyal, P., Sereda, J., and Lindenschmidt, K.: Changes in streamflow and water temperature affect fish habitat in the Athabasca River basin in the context of climate change, Ecological Modelling, 407, 108 718, https://doi.org/10.1016/j.ecolmodel.2019.108718, 2019.

Morel, M., Booker, D. J., Gob, F., and Lamouroux, N.: Intercontinental predictions of river hydraulic geometry from catchment physical characteristics, Journal of Hydrology, 582, 124 292, https://doi.org/10.1016/j.jhydrol.2019.124292, 2020.

730 Nash, J. E. and Sutcliffe, J. V.: River Flow Forecasting Through Conceptual Models. Part 1: A Discussion of Principles, Journal of Hydrology, 10, 282–290, https://doi.org/10.1016/0022-1694(70)90255-6, 1970.

Nelson, K. C. and Palmer, M. A.: Stream temperature surges under urbanization and climate change: data, models, and responses 1, JAWRA Journal of the American Water Resources Association, 43, 440–452, https://doi.org/10.1111/j.1752-1688.2007.00034.x, 2007.

Niedrist, G. H. and Füreder, L.: Real-time warming of alpine streams:(Re) defining invertebrates' temperature preferences, River Research 735 and Applications, 37, 283–293, https://doi.org/10.1002/rra.3638, 2021.

O'Gorman, E. J., Pichler, D. E., Adams, G., Benstead, J. P., Cohen, H., Craig, N., Cross, W. F., Demars, B. O., Friberg, N., Gislason, G. M., et al.: Impacts of warming on the structure and functioning of aquatic communities: individual-to ecosystem-level responses, Advances in ecological research, 47, 81–176, https://doi.org/10.1016/B978-0-12-398315-2.00002-8, 2012.

Olden, J. D. and Naiman, R. J.: Incorporating thermal regimes into environmental flows assessments: modifying dam operations to restore 740 freshwater ecosystem integrity, Freshwater Biology, 55, 86–107, https://doi.org/10.1111/j.1365-2427.2009.02179.x, 2010.

Orr, H. G., Simpson, G. L., des Clers, S., Watts, G., Hughes, M., Hannaford, J., Dunbar, M. J., Laizé, C. L., Wilby, R. L., Battarbee, R. W., et al.: Detecting changing river temperatures in England and Wales, Hydrological Processes, 29, 752–766, https://doi.org/10.1002/hyp.10181, 2015.

Palmer, M. A., Lettenmaier, D. P., Poff, N. L., Postel, S. L., Richter, B., and Warner, R.: Climate change and river ecosystems: protection and 745 adaptation options, Environmental management, 44, 1053–1068, https://doi.org/10.1007/s00267-009-9329-1, 2009.

Pella, H., Lejot, J., Lamouroux, N., and Snelder, T.: Le réseau hydrographique théorique (RHT) français et ses attributs environnementaux, Géomorphologie: relief, processus, environnement, 18, 317–336, https://doi.org/10.4000/geomorphologie.9933, 2012.

Perry, L. G., Reynolds, L. V., Beechie, T. J., Collins, M. J., and Shafroth, P. B.: Incorporating climate change projections into riparian restoration planning and design, Ecohydrology, 8, 863–879, https://doi.org/10.1002/eco.1645, 2015.

750 Pettitt, A. N.: A non-parametric approach to the change-point problem, Applied Statistics, 28, 126–135, https://doi.org/10.2307/2346729, 1979.

Poole, G. C. and Berman, C. H.: An ecological perspective on in-stream temperature: natural heat dynamics and mechanisms of human-causedthermal degradation, Environmental management, 27, 787–802, https://doi.org/10.1007/s002670010188, 2001.

Prudhomme, C., Giuntoli, I., Robinson, E. L., Clark, D. B., Arnell, N. W., Dankers, R., Fekete, B. M., Franssen, W., Gerten, D., Gosling, S. N., 755 et al.: Hydrological droughts in the 21st century, hotspots and uncertainties from a global multimodel ensemble experiment, Proceedings of the National Academy of Sciences, 111, 3262–3267, https://doi.org/10.1073/pnas.1222473110, 2014.

Ptak, M., Choiński, A., and Kirviel, J.: Long-term water temperature fluctuations in coastal rivers (southern Baltic) in Poland, Bulletin of Geography. Physical Geography Series, 11, 35–42, https://doi.org/10.1515/bgeo-2016-0013, 2016.

Ptak, M., Sojka, M., Kałuża, T., Choiński, A., and Nowak, B.: Long-term water temperature trends of the Warta River in the years 1960–2009, 760 Ecohydrology & Hydrobiology, 19, 441–451, https://doi.org/10.1016/j.ecohyd.2019.03.007, 2019a.

Ptak, M., Sojka, M., and Kozłowski, M.: The increasing of maximum lake water temperature in lowland lakes of Central Europe: case study of the Polish Lakeland, in: Annales de Limnologie-International Journal of Limnology, vol. 55, p. 6, EDP Sciences, https://doi.org/10.1051/limn/2019005, 2019b.

Quintana-Segui, P., Le Moigne, P., Durand, Y., Martin, E., Habets, F., Baillon, M., Canellas, C., Franchisteguy, L., and Morel, S.: Analysis of near-surface atmospheric variables: Validation of the SAFRAN analysis over France, Journal of applied meteorology and climatology, 47, 92–107, https://doi.org/10.1175/2007JAMC1636.1, 2008.

Romaní, A. M., Boulêtreau, S., Villanueva, V. D., Garabetian, F., Marxsen, J., Norf, H., Pohlon, E., Weitere, M., et al.: Microbes in aquatic biofilms under the effect of changing climate., Climate change and microbial ecology: Current research and future trends, pp. 83–96, 2016.

Sanchez-Lorenzo, A., Wild, M., Brunetti, M., Guijarro, J. A., Hakuba, M. Z., Calbó, J., Mystakidis, S., and Bartok, B.: Reassessment and update of long-term trends in downward surface shortwave radiation over Europe (1939–2012), Journal of Geophysical Research: Atmospheres, 120, 9555–9569, https://doi.org/10.1002/2015JD023321, 2015.

Scheffers, B. R., De Meester, L., Bridge, T. C., Hoffmann, A. A., Pandolfi, J. M., Corlett, R. T., Butchart, S. H., Pearce-Kelly, P., Kovacs, K. M., Dudgeon, D., et al.: The broad footprint of climate change from genes to biomes to people, Science, 354, https://doi.org/10.1126/science.aaf7671, 2016.

Seavy, N. E., Gardali, T., Golet, G. H., Griggs, F. T., Howell, C. A., Kelsey, R., Small, S. L., Viers, J. H., and Weigand, J. F.: Why climate change makes riparian restoration more important than ever: recommendations for practice and research, Ecological Restoration, 27, 330–338, https://doi.org/10.3368/er.27.3.330, 2009.

Sen, P. K.: Estimates of the regression coefficient based on Kendall's tau, Journal of the American statistical association, 63, 1379–1389, https://doi.org/10.1080/01621459.1968.10480934, 1968.

Seyedhashemi, H., Moatar, F., Vidal, J.-P., Diamond, J. S., Beaufort, A., Chandesris, A., and Valette, L.: Thermal signatures identify the influence of dams and ponds on stream temperature at the regional scale, Science of The Total Environment, p. 142667, https://doi.org/10.1016/j.scitotenv.2020.142667, 2020.

Sinokrot, B., Stefan, H., McCormick, J., and Eaton, J.: Modeling of climate change effects on stream temperatures and fish habitats below dams and near groundwater inputs, Climatic Change, 30, 181–200, https://doi.org/10.1007/BF01091841, 1995.

Spinoni, J., Naumann, G., and Vogt, J. V.: Pan-European seasonal trends and recent changes of drought frequency and severity, Global and Planetary Change, 148, 113–130, https://doi.org/10.1016/j.gloplacha.2016.11.013, 2017.

Stefan, H. G. and Preud'homme, E. B.: Stream temperature estimation from air temperature 1, JAWRA Journal of the American Water Resources Association, 29, 27–45, https://doi.org/10.1111/j.1752-1688.1993.tb01502.x, 1993.

Stefani, F., Schiavon, A., Tirozzi, P., Gomarasca, S., and Marziali, L.: Functional response of fish communities in a multistressed freshwater world, Science of The Total Environment, 740, 139 902, https://doi.org/10.1016/j.scitotenv.2020.139902, 2020.

Taylor, C. A. and Stefan, H. G.: Shallow groundwater temperature response to climate change and urbanization, Journal of Hydrology, 375, 601–612, https://doi.org/10.1016/j.jhydrol.2009.07.009, 2009.

Thiéry, D.: Forecast of changes in piezometric levels by a lumped hydrological model, Journal of Hydrology, 97, 129–148, https://doi.org/10.1016/0022-1694(88)90070-4, 1988.

Thiéry, D.: Logiciel ÉROS version 7.1. Guide d'utilisation, in: Rapport BRGM/RP-67704-FR, http://infoterre.brgm.fr/rapports/RP-67704-FR.pdf, 2018.

Thiéry, D. and Moutzopoulos, C.: Un modèle hydrologique spatialisé pour la simulation de très grands bassins: le modèle EROS formé de grappes de modèles globaux élémentaires, VIIIèmes journées hydrologiques de l'ORSTOM" Régionalisation en hydrologie, application au développement", Le Barbé et E. Servat (Eds.), pp. 285–295, https://hal-brgm.archives-ouvertes.fr/hal-01061971, 1995.

Tisseuil, C., Vrac, M., Grenouillet, G., Wade, A. J., Gevrey, M., Oberdorff, T., Grodwohl, J.-B., and Lek, S.: Strengthening the link between climate, hydrological and species distribution modeling to assess the impacts of climate change on freshwater biodiversity, Science of the total environment, 424, 193–201, https://doi.org/10.1016/j.scitotenv.2012.02.035, 2012.

Tramblay, Y., Koutroulis, A., Samaniego, L., Vicente-Serrano, S. M., Volaire, F., Boone, A., Le Page, M., Llasat, M. C., Albergel, C., Burak, S., Cailleret, M., Cindrić Kalin, K., Davi, H., Dupuy, J.-L., Greve, P., Grillakis, M., Hanich, L., Jarlan, L., Martin-StPaul, N., Martínez-Vilalta, J., Mouillot, F., Pulido-Velazquez, D., Quintana-Seguí, P., Renard, D., Turco, M., Türkeş, M., Trigo, R., Vidal, J.-P., Vilagrosa, A., Zribi, M., and Polcher, J.: Challenges for drought assessment in the Mediterranean region under future climate scenarios, Earth-Science Reviews, 210, 103 348, https://doi.org/10.1016/j.earscirev.2020.103348, 2020.

Valette, L., Piffady, J., Chandesris, A., and Souchon, Y.: SYRAH-CE: description des données et modélisation du risque d'altération hydromorphologique des cours d'eau pour l'état des lieux DCE, Rapport Technique Onema-Irstea, http://oai.afbiodiversite.fr/cindocoai/download/PUBLI/1185/1/2012_108.pdf_4080Ko, 2012.

van Looy, K. and Tormos, T.: Indicateurs spatialisés du fonctionnement des corridors rivulaires, Tech. rep., Irstea, https://hal.inrae.fr/hal-02599341, 2013.

Van Vliet, M., Ludwig, F., Zwolsman, J., Weedon, G., and Kabat, P.: Global river temperatures and sensitivity to atmospheric warming and changes in river flow, Water Resources Research, 47, https://doi.org/10.1029/2010WR009198, 2011.

van Vliet, M. T., Franssen, W. H., Yearsley, J. R., Ludwig, F., Haddeland, I., Lettenmaier, D. P., and Kabat, P.: Global river discharge and water temperature under climate change, Global Environmental Change, 23, 450–464, https://doi.org/10.1016/j.gloenvcha.2012.11.002, 2013.

Vicente-Serrano, S., Hannaford, J., Murphy, C., Peña Gallardo, M., Lorenzo-Lacruz, J., Domínguez-Castro, F., López Moreno, J. I., Beguería, S., Noguear, I., Harrigan, S., and Vidal, J.-P.: Climate, irrigation, and land-cover change explain streamflow trends in countries bordering the Northeast Atlantic, Geophysical Research Letters, 46, 10 821–10 833, https://doi.org/10.1029/2019GL084084, 2019.

Vidal, J.-P., Martin, E., Franchistéguy, L., Baillon, M., and Soubeyroux, J.-M.: A 50-year high-resolution atmospheric reanalysis over France with the Safran system, International Journal of Climatology, 30, 1627–1644, https://doi.org/10.1002/joc.2003, 2010.

Vidal, J.-P., Hingray, B., Magand, C., Sauquet, E., and Ducharne, A.: Hierarchy of climate and hydrological uncertainties in transient low-flow projections, Hydrology and Earth System Sciences, 20, 3651–3672, https://doi.org/https://doi.org/10.5194/hess-20-3651-2016, 2016.

Wanders, N., van Vliet, M. T., Wada, Y., Bierkens, M. F., and van Beek, L. P.: High-resolution global water temperature modeling, Water Resources Research, 55, 2760–2778, https://doi.org/10.1029/2018WR023250, 2019.

Wasson, J.-G., Chandesris, A., Pella, H., and Blanc, L.: Typology and reference conditions for surface water bodies in France: the hydro-ecoregion approach, TemaNord, 566, 37–41, https://hal.archives-ouvertes.fr/hal-00475620/document, 2002.

Webb, B.: Trends in stream and river temperature, Hydrological processes, 10, 205–226, https://doi.org/10.1002/(SICI)1099-1085(199602)10:2<205::AID-HYP358>3.0.CO;2-1, 1996.

Webb, B. and Walling, D.: Long-term variability in the thermal impact of river impoundment and regulation, Applied Geography, 16, 211–223, https://doi.org/10.1016/0143-6228(96)00007-0, 1996.

Webb, B. and Walling, D.: Complex summer water temperature behaviour below a UK regulating reservoir, Regulated Rivers: Research & Management: An International Journal Devoted to River Research and Management, 13, 463–477, https://doi.org/10.1002/(SICI)1099-1646(199709/10)13:5<463::AID-RRR470>3.0.CO;2-1, 1997.

Webb, B. W., Hannah, D. M., Moore, D. R., Brown, L. E., and Nobilis, F.: Recent advances in stream and river temperature research, Hydrological Processes: An International Journal, 22, 902–918, https://doi.org/10.1002/hyp.6994, 2008.

Wilby, R. and Johnson, M.: Climate variability and implications for keeping rivers cool in England, Climate Risk Management, 30, 100 259, https://doi.org/10.1016/j.crm.2020.100259, 2020.

Wondzell, S. M., Diabat, M., and Haggerty, R.: What matters most: are future stream temperatures more sensitive to changing air temperatures, discharge, or riparian vegetation?, JAWRA Journal of the American Water Resources Association, 55, 116–132, https://doi.org/10.1111/1752-1688.12707, 2019.

Woodward, G., Perkins, D. M., and Brown, L. E.: Climate change and freshwater ecosystems: impacts across multiple levels of organization, Philosophical Transactions of the Royal Society B: Biological Sciences, 365, 2093–2106, https://doi.org/10.1098/rstb.2010.0055, 2010.

Yearsley, J. R.: A semi-Lagrangian water temperature model for advection-dominated river systems, Water Resources Research, 45, https://doi.org/10.1029/2008WR007629, 2009.

Zaidel, P. A., Roy, A. H., Houle, K. M., Lambert, B., Letcher, B. H., Nislow, K. H., and Smith, C.: Impacts of small dams on stream temperature, Ecological Indicators, 120, 106 878, https://doi.org/10.1016/j.ecolind.2020.106878, 2020.

Zhu, S., Bonacci, O., Oskoruš, D., Hadzima-Nyarko, M., and Wu, S.: Long term variations of river temperature and the influence of air temperature and river discharge: case study of Kupa River watershed in Croatia, Journal of Hydrology and Hydromechanics, 67, 305–313, https://doi.org/10.2478/johh-2019-0019, 2019.

Zobrist, J., Schoenenberger, U., Figura, S., and Hug, S. J.: Long-term trends in Swiss rivers sampled continuously over 39 years reflect changes in geochemical processes and pollution, Environmental Science and Pollution Research, 25, 16 788–16 809, https://doi.org/10.1007/s11356-018-1679-x, 2018.

Table 1. Characteristics of the 14 long-term Tw stations. See Fig. S1 S4 for the evolution of observed annual Tw at these stations. The ID of stations correspond to the numbers (in red) shown in the Fig. 1, middle. The coordinate system is Lambert 93.

ID	River (Location)	Catchment area (km^2)	Record period	Total years	Source of data	X	Y
1	Loire (Chinon)	57043	1977–2019	43	EDF	493337	6688043
2	Loire (St-Laurent)	38088	1977-2019	43	EDF	596822	6737144
3	Loire (Dampierre)	36212	1977–2019	43	EDF	663009	6736208
4	Loire (Bellevile)	35172	1979–2019	41	EDF	691553	6712421
5	Vienne (Civaux)	5795	1997–2017	21	EDF	521421	6596684
6	Artière (Clermont-Ferrand)	48	2005–2017	13	DREAL Auvergne	710982	6519098
7	Oudon (Segré)	1342	2004–2014	11	DREAL PDL	410465	6738872
8	Mayenne (Ambrières-les-Vallées)	825	2004–2014	11	DREAL PDL	434920	6822096
9	Bedat (Saint-Laure)	419	2008–2017	10	DREAL Auvergne	722677	6533379
10	Credogne (Puy-Guillaume)	84	2008–2017	10	DREAL Auvergne	736684	6540613
11	Loir (Flée)	6215	2010–2017	8	DREAL PDL	511117	6737501
12	Huisne (Montfort-le-Gesnois)	1931	2010–2017	8	DREAL PDL	506734	6774430
13	Jouanne (Forcé)	413	2010–2017	8	DREAL PDL	423991	6776828
14	Merdereau (Saint-Paul-le-Gaultier)	123	2010-2017	8	DREAL PDL	466815	6808016

Table 2. Pearson correlation over the 1963–2019 period between seasonal and annual Tw and Ta and/or ~~log-transformed~~ Q time series, averaged over all reaches. Percentages in brackets show the proportion of reaches with a significant correlation at the 95 % confidence level.

Season	Tw and Ta	Tw and ~~log(Q)~~Q
DJF	+0.73 (100%)	+0.52 (94%)
MAM	+0.78 (100%)	-0.02 (25%)
JJA	+0.82 (100%)	-0.40 (79%)
SON	+0.72 (~~99,6~~99.6%)	-0.01 (19%)
Annual	+0.83 (100%)	-0.01 (22%)

Table 3. Recent studies on Tw trends in Europe. A comprehensive review of the relevant literature published prior to 2016 can be found in Arora et al. (2016). Magnitudes with unspecified season are related to annual scale. Notice that except present study, the others used observed Tw.

Country	Sites	Period	Rate of change (°C/decade)	Reference
France	**52 278 reaches in the Loire basin**	**1963–2019**	**+0.17 to +0.72 (Mean=+0.38)**	**Present study**
			+0.01 to +0.65 (+0.35) in winter	
			+0.11 to +0.76 (+0.38) in spring	
			+0.08 to +1.02 (+0.44) in summer	
			+0.05 to +0.81 (+0.33) in fall	
Austria	18 rivers	2010-2017	+1.9 to +3.2 in summer	Niedrist and Füreder (2021)
England	6148 sites	2000-2018	-0.4	Wilby and Johnson (2020)
Switzerland	31 rivers	1979-2018	+0.33 (±0.03)	Michel et al. (2020)
			+0.6 to +1.1 in summer	
Poland	5 Carpathian rivers	1984–2018	+0.33 to +0.92	Kędra (2020)
			+0.82 to +0.95 in spring	
			+0.75 to +1.17 in summer	
			+0.51 to +1.08 in fall	
			+0.25 to +0.29 in winter	
France	11 stations on Loire, Vienne, Rhône, Seine, Meuse	1980-2015	+0.79 in spring	Maire et al. (2019)
Poland	6 stations on Warta River	1960-2009	+0.096 to +0.28	Ptak et al. (2019a)
Croatia	6 stations on Kupa River	1990-2017	+0.23 to +0.796	Zhu et al. (2019)
Switzerland	Rhine, Rhône, Aar, and Thur rivers	1983-2013	+0.27 (± 0.03)	Zobrist et al. (2018)
Northern Germany	132 sites	1985-2010	+0.3 (±0.03)	Arora et al. (2016)
		1985-1995	+0.69 (±0.10) in spring	
			+0.78 (±0.06) in summer	
			+0.75 (±0.09) in fall	
			+0.39 (±0.23) in winter	
			+0.81 (±0.2)	
	475 sites	2000-2010	+0.9 (±0.07)	
England and Wales	2773 sites	1990–2006	+0.3 (±0.02)	Orr et al. (2015)
Poland	Coastal rivers (Rega, Parsęta, Słupia, Łupawa, Łeba)	1971-2015	+0.26 to +0.31	Ptak et al. (2016)
			+0.46 in April (the month with the highest trend)	
France	4 stations on Loire River	1976–2003	+0.61 to +0.71	Moatar and Gailhard (2006)
			+0.86 to +1.07 in spring and summer	